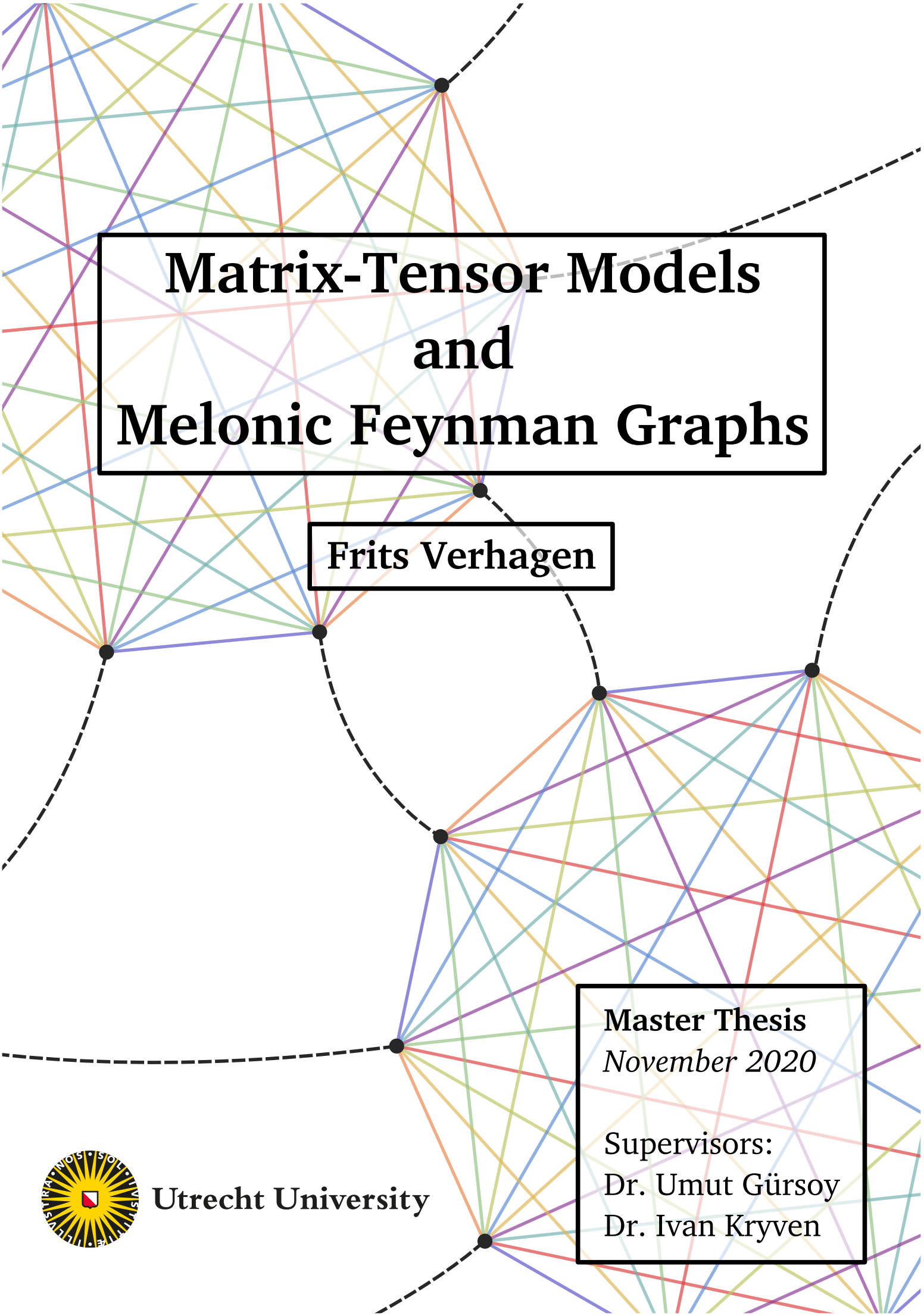

Matrix-Tensor Models and Melonic Feynman Graphs

Frits Verhagen

Master Thesis
November 2020

Supervisors:
Dr. Umut Gürsoy
Dr. Ivan Kryven

Utrecht University

Title

Matrix-Tensor Models and Melonic Feynman Graphs

Author

Frits Verhagen
Mathematical Institute and Institute for Theoretical Physics
Utrecht University

Supervisors

Dr. Umut Gürsoy
Institute for Theoretical Physics
Utrecht University

Dr. Ivan Kryven
Mathematical Institute
Utrecht University

Image on the Cover

Here we see two copies of the unique (up to isomorphism) MST coloring of the complete graph with 10 vertices, also known as the perfect 1-factorization of this graph. These two copies represent two interaction vertices in a Feynman graph, and they are connected by propagators (dashed lines) in a way that is consistent with Lemma 4.8.

Abstract

Matrix-tensor models give rise to a special type of Feynman graphs: the melonic graphs. These graphs can all be obtained by repeatedly inserting a melon, which is a certain fundamental building block, onto propagators in the graph. Matrix-tensor models are connected to the quantum mechanical description of black holes.

In this thesis, we first introduce matrix-tensor models and their properties. Then, we present a new set of interaction terms - the so-called MST interactions on a complete graph - and prove that all the associated Feynman graphs are melonic.

Also, we introduce a new limiting procedure that in certain cases selects not only the melonic graphs, but also graphs that can be embedded into surfaces of higher genus. Finally, we discuss two combinatorial approaches to computing the two-point function in theories with melonic graphs.

Contents

1 Introduction

Since the theoretical discovery of the possibility of black holes following from Einstein's general theory of relativity, people have tried to confirm if these objects actually exist in the universe. In the last ~100 years we have gained more theoretical and observational evidence and we can be quite sure that black holes exist. The 2020 Nobel Prize in physics was awarded to mark these achievements. The next step in the study of black holes is to consider them in a quantum mechanical setting, which is an ongoing subject of study in the theory of quantum gravity and string theory.

One model for quantum gravity are the so-called tensor models, whose study goes back to the study of matrix models by Gerard 't Hooft in the 1970's. If N is the number of tensor indices and we take the limit $N \to \infty$, then these tensor models yield a specific type of Feynman graphs: the melonic graphs. These graphs have a simple description: they can all be built in an inductive way by repeatedly inserting a so-called melon - a "fundamental building block" - onto propagators in a Feynman graph. In this way, one obtains all the possible Feynman graphs. See Figure 1.1.

In 2015, Alexei Kitaev [5] proposed another model that exhibited properties of a quantum black hole: the Sachdev-Ye-Kitaev (SYK) model. This model has the disadvantage that it has quenched-disorder, meaning that the coupling constants are in fact not constant, but are drawn from a probability distribution. Also, the connection with this model to quantum gravity is not clear. It was noticed by Edward Witten in 2017 [11] that the SYK model and tensor models in the limit $N \to \infty$ both yield melonic Feynman graphs. Since the connection with quantum gravity in the tensor models was more clear, he suggested that these tensor models could provide a better model for quantum black holes.

In this thesis we treat a special type of tensor model, the matrix-tensor model, introduced by Frank Ferrari et al. [3], [4]. Here, we use tensors where we differentiate between two different types of indices: two indices take values in $1, \ldots, N$ and the other indices take values in $1, \ldots, D$. We can use different interaction terms in this model, and when we choose so-called MST terms we get melonic Feynman graphs in the limit $N, D \to \infty$. However, there can also be non-melonic Feynman graphs that

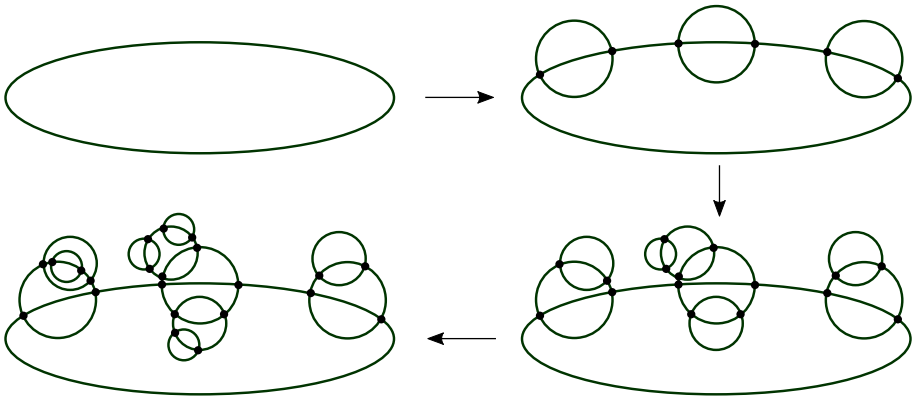

Figure 1.1: Melonic Feynman graphs. Starting from a single propagator loop (upper left), we repeatedly insert so-called melons onto propagators to obtain all the possible Feynman graphs.

need to be taken into account. We describe and prove a new result, namely that for the class of MST interaction terms on the complete graph, the melonic graphs give a complete description of the Feynman graphs involved.

Chapter 2 introduces concepts about (colored) graphs and their embeddings, which we will need in the rest of the thesis. In Chapter 3, we explain what the matrix-tensor model is and what the important properties are. Chapter 4 is the central part of this thesis. Here we prove our result about a class of interaction terms that give melonic Feynman graphs. Chapter 5 analyses a new large N, D limit and the consequences this has for the Feynman graphs. Finally, in Chapter 6, we present two different combinatorial methods to compute the two-point function in theories that have melonic Feynman graphs.

2 Mathematical Preliminaries

In this chapter we cover some mathematical preliminaries that are used in the rest of the thesis. Section 2.1 introduces some concepts about (colored) graphs. Section 2.2 explains how we can embed graphs into surfaces.

2.1 Colored Graphs

Here we collect some basic definitions about graphs, as well as some more specific notions that are used in this thesis. We start by giving a precise definition of a graph.

Definition 2.1. A *graph* G is a pair (V, E), where V is a finite set of *vertices* (singular: *vertex*) and E a finite set of *edges*, such that each edge $e \in E$ is associated with two distinct vertices $v_1, v_2 \in V$. We say that e is *incident* on v_1 and v_2, that v_1 and v_2 are *adjacent*, and we write $e = v_1v_2$ or $e = v_2v_1$. The *order* of a vertex v is the number of edges incident on v.

Note that we allow multiple edges to be incident on a pair of vertices. In some texts, this type of graph is referred to as a multigraph.

Definition 2.2. A *colored* graph $\mathcal{G}$ is a graph G together with a set of *colors*, usually taken to be $\{1, \ldots, r\}$, and an assignment of a color to each edge of G.

Definition 2.3. A *walk* in a graph G is an ordered sequence $v_1, e_1, v_2, \ldots, e_k, v_{k+1}$ of alternately vertices v_i and edges e_i in G such that each edge is incident on the preceding vertex and subsequent vertex. We say that the walk *visits* the vertices and edges in the walk and the walk has *length* k. For a colored graph, a walk is denoted by:

$$v_1 \overset{c_1}{-} v_2 \overset{c_2}{-} \cdots \overset{c_k}{-} v_{k+1}, \tag{2.1}$$

where $c_1, \ldots, c_k$ are the colors of the corresponding edges.

A *path* is a walk where no vertices, except possibly the first and last, are repeated (and hence also no edges are repeated). A *cycle* is a path where the first and last

vertex are the same. For a colored graph $\mathcal{G}$ and two distinct colors i, j an (ij)-*face* is a cycle in $\mathcal{G}$ such that the color of the visited edges alternate between i and j:

$$v_1 \overset{i}{-} v_2 \overset{j}{-} v_3 \overset{i}{-} \cdots v_1. \tag{2.2}$$

The number of distinct (ij)-faces in $\mathcal{G}$ is denoted by $F_{ij}(\mathcal{G})$.

The reason for using the term "faces" is that these correspond to the faces of an embedding of the graph, as we will see further on.

Definition 2.4. We say that two vertices, two edges, respectively one edge and one vertex, in a graph G are *connected* if there exists a walk that visits the two vertices, two edges, respectively the edge and the vertex. A *connected component* of G is a set of vertices and edges C that are pairwise connected, such that there is no set C' with the same property for which $C \subsetneq C'$. The number of distinct connected components is denoted by $c(G)$. If there is only one connected component, the graph is called *connected*.

Definition 2.5. A graph is called k-*regular* if every vertex has precisely k edges incident on it and *complete* if every vertex is adjacent to every other vertex. A *bubble* is an r-regular colored graph, where r is the number of colors, such that every vertex has precisely one edge of every color incident on it.

Bubbles will be the type of graph we deal with the most in this thesis, since Feynman graphs are bubbles.

2.2 Graph Embeddings, the Genus and Euler's Formula

This section discusses how to embed a connected graph onto a surface, or in other words how to draw a connected graph on a surface such that no edges overlap. We explain what the surfaces are onto which we can embed connected graphs. These surfaces can be characterized by their genus, a non-negative half-integer. We explain that the genus is related to some combinatorial properties of the graph via Euler's formula. In this section many statements will not be proved, since this would require a much longer exposition and it is not essential to the rest of the thesis. However, an intuitive understanding of these concepts is useful and therefore we will focus on that. We refer to Chapters 3 and 4 in [6] for proofs and more details about some notions we discuss here.

The Orientable and Non-Orientable Surfaces We start with the unit sphere in $\mathbb{R}_3$, denoted by S_0, and perform one of two operations on S_0 to obtain other surfaces. The first operation is inserting a *handle*, pictured in Figure 2.1 (a). Here, the gray area represents a part of the surface of S_0. We remove two disks from the surface and glue the two circular edges onto each other, in such a way that the directions of the two arrows agree. One sees that we indeed get a sphere with a handle attached in this way, which is (homeomorphic to) the torus. We can perform

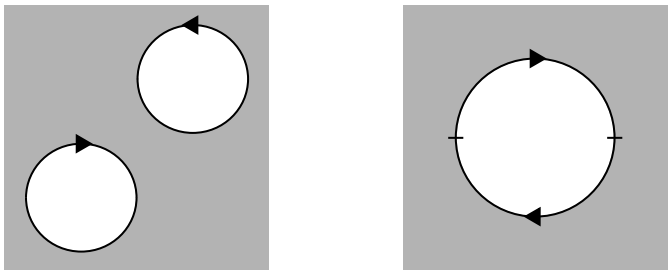

(a) (b)

Figure 2.1: The gray areas represent part of a surface. (a): A handle. The two circular edges should be glued to each other, respecting the orientation of the arrows. (b): A crosscap. Here, the two edges shaped as half-circles should be glued, respecting the orientation of the arrows.

this insertion of a handle multiple times on S_0 and the surface obtained after k handle insertions is denoted by S_k. The surfaces S_k are called *orientable* and S_1 is the torus, S_2 the double torus et cetera.

The second operation on S_0 is inserting a *crosscap*, pictured in Figure 2.1 (b). Here, the gray area represents a part of the surface of S_0 and we remove one disk from the surface. Then, we glue all points on the circular edge that are on opposite sides of the sphere. Or equivalently, we glue the two halves of the edge onto each other, such that the directions of the two arrows agree, as in the figure. Note that this surface cannot exist as a physical object in $\mathbb{R}^3$, but it is known that it is possible to embed it in $\mathbb{R}^4$. However, the topological space is well-defined by the gluing instructions, i.e. the identification of the points on the edge as we described. As with the handle, one can insert the crosscap multiple times on S_0. The surface obtained after k crosscap insertions is denoted by N_k. The surfaces N_k are called *non-orientable* and N_1 is known as the projective plane and N_2 as the Klein bottle.

We define the *genus* of S_g as the integer g, and of S_{2g} as the (half-)integer g.

Graph Embeddings Let G be a connected graph with vertex set V and edge set E. For every $v \in V$ fix a cyclic permutation π_v of the edges incident on v, i.e. $\pi_v = (e_1 e_2 \cdots e_m)$, where $e_1, e_2, \ldots, e_m$ are all the edges incident on v. The set $\pi = \{\pi_v : v \in V\}$ is called a *rotation system*. To each $e \in E$ associate a *sign* $\lambda(e) = 1$ or $\lambda(e) = -1$. The resulting map $\lambda\colon E \to \{-1, 1\}$ is called a *signature*. The pair (π, λ) is called an *embedding*, for reasons we explain next.

Let $\Pi = (\pi, \lambda)$ be an embedding of a connected graph G, v_1 a vertex of G and e_1 an edge incident on v. First, assume that λ is equal to 1 at all edges. The general case will be treated next. Define the walk $v_1, e_1, v_2, e_2, \ldots, v_k, e_k, v_1$ as follows. Start with v_1 and continue along e_1, to reach vertex v_2. Then continue along the edge $e_2 = \pi_{v_2}(e_1)$, to reach vertex v_3. Then continue along $e_3 = \pi_{v_3}(e_2)$ and repeat this procedure until we reach v_1 again *and* $\pi_{v_1}(e_k) = e_1$, where e_k is the edge preceding v_1. To see that this is well-defined, i.e. that we traverse e_1 for a second time in the same direction, note the following: since G is finite we eventually traverse some

edge in the same direction for a second time, and one checks that the first edge that we traverse in the same direction for a second time must be e_1. The walk defined this way is called a Π-*face*.

In the general case where λ is not necessarily equal to 1 at all edges we define a Π-face in a slightly different way. We start at v_1 in a positive *mode*. Every time we traverse an edge e with $\lambda(e) = -1$ the mode is changed from positive to negative or vice versa. When we traverse an edge e and reach a vertex v while in a negative mode, we continue along the edge $\pi_v^{-1}(e)$. When reaching a vertex in a positive mode we proceed along $\pi_v(e)$. Repeat this procedure until we reach v_1 again while in the positive mode *and* $\pi_{v_1}(e_k) = e_1$, where e_k is the edge preceding v_1. One checks similarly as before that this is well-defined.

By starting with different vertices v_1 and incident edges e_1 we obtain all the Π-faces of G (note that different choices of v_1, e_1 may yield the same walk, up to a cyclic shift, but we consider the resulting Π-face to be the same). One can check that each edge in G is either contained once in two distinct Π-faces, or contained twice in a single Π-face.

Next, for every Π-face we take a polygon (including its interior) with k edges, where k is the number of edges (edges repeated twice are counted twice) in the Π-face. These polygons are also called *faces* in the embedding. Consider all the polygons we obtain from the Π-face. Every edge in a polygon has two corners of the polygon at its ends, which correspond to vertices in the original graph. Each edge in G corresponds to two edges in two distinct polygons or in a single polygon. We glue these two edges together, orienting the polygon(s) such that each of the corners of the glued edges are glued to a corner corresponding to the same vertex in G. In this way, we obtain a connected surface and we say that the graph is *embedded* in the surface. This surface is (homeomorphic to) one of the surfaces S_k or N_k introduced above, which is the content of the following theorem. See Chapters 3 and 4 in [6] for a proof.

Theorem 2.6. *The surface into which a connected graph is embedded is either one of the orientable surfaces S_g for $g = 0, 1, \ldots$ or one of the non-orientable surfaces N_g for $g = \frac{1}{2}, \frac{3}{2}, \ldots$.*

Figure 2.2, in the middle column, shows the faces obtained in three different embeddings of K_4. The embedding used is encoded in the so-called ribbon graphs in the first column, which will be explained in the next section. We leave it as an exercise to check that gluing these polygons using the procedure described above yields the surface in the last column. In this column, the edges with the same type of arrow are glued, respecting the direction of the arrows.

If a connected graph G has an embedding into a surface with genus g and this choice of embedding is clear from the context, we say that G has genus g and denote the genus by $g(G)$. When a graph G has multiple connected components (i.e. is not connected) we can have an embedding for each connected component and we define the genus of G as the sum of the genera of these connected components. We refer to the embeddings of the connected components together as *the* embedding of G.

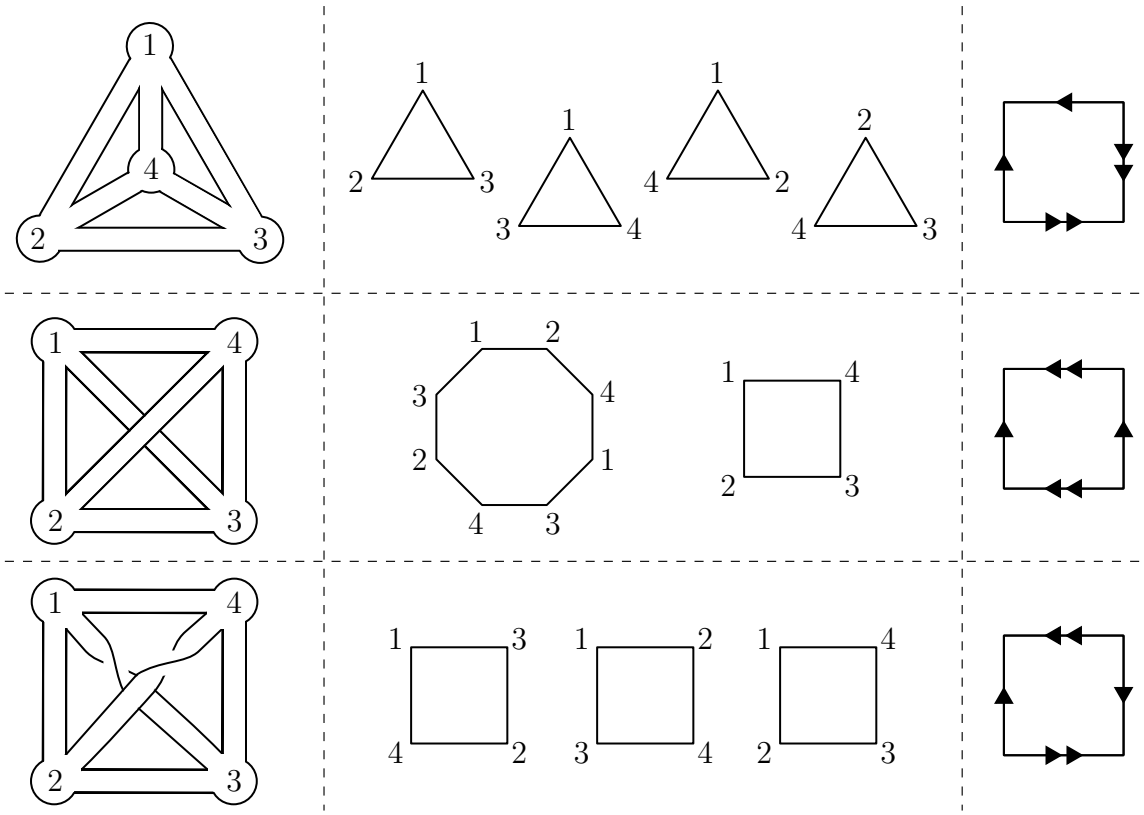

Figure 2.2: Three different embeddings of K_4. The left column shows the ribbon graphs. The middle column shows the faces in the embedding. The corners of the faces are glued such that the labels of the vertices match up. The right column shows the result of gluing these faces together. Here, the edges with the same type of arrow are glued, respecting the direction of the arrows. The resulting surfaces are, from top to bottom: the sphere ($g = 0$), the torus ($g = 1$) and the projective plane ($g = 1/2$).

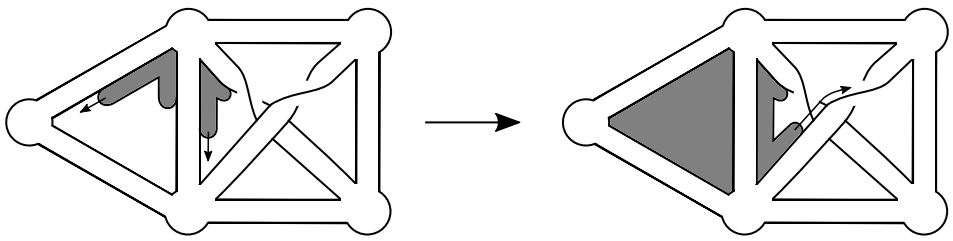

Figure 2.3: Illustration of obtaining the surface in which a graph is embedded by "rolling a disk" along all the edges of the ribbon graph. The gray areas are the disks and the arrows near the gray areas indicate the direction they are rolled.

There is a relation between the genus of a graph, the number of vertices and edges of the graph, and the number of faces of the embedding. This relation is known as Euler's Formula and is given below. See Chapters 3 and 4 in [6] for a proof.

Theorem 2.7 (Euler's Formula)**.** *Let G be a graph with genus g. Denote by V the number of vertices of G, E the number of edges and F the number of faces in the embedding. Then:*

$$2c(G) - 2g = V - E + F. \tag{2.3}$$

One can check that this relation is satisfied in the examples in Figure 2.2.

Ribbon Graphs A *ribbon graph* is a topological space obtained from a graph G with an embedding (Π, λ) as follows. Every vertex is represented by a disk that has a front and back side, and every edge by a rectangle called a *ribbon*. To each vertex v is associated a counterclockwise ordering of the incident edges $e, \pi_v(e), \pi_v^2(e), \ldots, e$, where e is one of the incident edges. For each edge and the vertices it is incident on, glue two sides of the corresponding ribbon to the sides of the corresponding disks, such that:

1. For an edge e, if $\lambda(e) = -1$ the corresponding ribbon is twisted, and untwisted if $\lambda(e) = 1$. With twisted we mean that when moving over a twisted ribbon from the front side of one disk, one arrives at the back side of the other disk. Moving over an untwisted ribbon one stays on the same side.

2. The counterclockwise ordering of the ribbons attached to every disk, when viewed from the front side, respect the counterclockwise ordering of the incident edges of the corresponding vertex.

See the left column of Figure 2.2 for the ribbon graphs corresponding to three different embeddings of K_4.

Ribbon graphs provide a convenient way to think of the surface a graph is embedded in, since we can use a ribbon graph to visualize the gluing process involved in obtaining the surface of the embedding in an intuitive way. Pick any ribbon in the ribbon graph and take a disk. We glue the disk to one of the edges of the ribbon and "roll" the disk along this edge and along the edges of all the subsequent disks associated with vertices and other ribbons. See Figure 2.3. Eventually we return back to where we started gluing the disk and in this we have removed one of the edges of the ribbon graph by gluing a face inside it. By gluing and rolling disks along the remaining edges we eventually glue all the faces and end up with a surface. One checks that this is the same surface obtained by the gluing process involved in defining the embedding of the graph. Note that although we cannot have non-orientable surfaces in $\mathbb{R}^3$, we can however have ribbon graphs in $\mathbb{R}^3$ yielding non-orientable surfaces. In this way, the ribbon graphs offer a way to visualize non-orientable surfaces.

No Intersection of Edges One sees that when there is an embedding of a graph into a surface, then one can draw this graph onto this surface, while respecting the chosen cyclic ordering of the incident edges of every vertex *and without any edges intersecting*. We will use this fact for $g = 0$ graph embeddings later.

3 Matrix-Tensor Models and Scaling

Here, we introduce the matrix-tensor model and derive a condition for the Feynman graphs that are selected by the large N, D limit. Our discussion is based on Sections 2 and 3 in [4].

3.1 Matrix-Tensor Models

We consider real $N \times N$-matrices $X_{\mu_1 \cdots \mu_r}$ labeled by r tensor indices μ_i, where each tensor index can take D different values, i.e. $\mu_i \in \{1, \ldots, N\}$. Notation:

$$(X_{\mu_1 \cdots \mu_r})_{ab} = X_{\mu_1 \cdots \mu_r ab}, \quad a, b = 1, \ldots, N \text{ and } \mu_i = 1, \ldots, D \text{ for } i = 1, \ldots, r. \tag{3.1}$$

Note that we can also consider $X_{\mu_1 \cdots \mu_r ab}$ to be a real tensor with $r+2$ indices, where the first r indices take D different values and the last two take N different values.

We will use the *Einstein summation convention*: in expressions involving these matrices we sum over all repeated indices, i.e. if an index appears twice in an expression we implicitly sum over this index while leaving out the summation sign. For example:

$$X_\mu X_\mu^T = \sum_{\mu=1}^{D} X_\mu X_\mu^T \tag{3.2}$$

$$X_{\mu\rho_1} X_{\nu\rho_2}^T X_{\mu\rho_3} X_{\nu\rho_4}^T = \sum_{\mu=1}^{D} \sum_{\nu=1}^{D} X_{\mu\rho_1} X_{\nu\rho_2}^T X_{\mu\rho_3} X_{\nu\rho_4}^T. \tag{3.3}$$

When we sum over an index in this way we say that the index is *contracted*.

The action of the matrix-tensor model is:

$$S = ND^r \left[\mathrm{tr}(X_{\mu_1 \ldots \mu_r} X_{\mu_1 \ldots \mu_r}^T) + \sum_a \tau_a I_a(X) \right]. \tag{3.4}$$

Here, the sum is over the interaction terms $I_a(X)$ and associated coupling constants τ_a that we include in the model. The interaction terms are of the following form:

$$I_a(X) = \mathrm{tr}(X_{\mu_1^{(1)} \cdots \mu_r^{(1)}} X^T_{\mu_1^{(2)} \cdots \mu_r^{(2)}} X_{\mu_3} X^T_{\mu_1^{(3)} \cdots \mu_r^{(3)}} \cdots X^T_{\mu_1^{(2k)} \cdots \mu_r^{(2k)}}), \tag{3.5}$$

where we multiply any even number of matrices and take the trace, and the indices are contracted pairwise in the following sense: each index $\mu_s^{(l)}$ in some matrix $X_{\mu_1^{(l)}\cdots\mu_r^{(l)}}$ or $X^T_{\mu_1^{(l)}\cdots\mu_r^{(l)}}$ above is contracted with the corresponding index $\mu_s^{(l')}$ in exactly one other matrix $X_{\mu_1^{(l')}\cdots\mu_r^{(l')}}$ or $X^T_{\mu_1^{(l')}\cdots\mu_r^{(l')}}$ ($l \neq l'$). Some examples of interaction terms:

$$\mathrm{tr}(X_\mu X_\nu^T X_\mu X_\nu^T), \quad \mathrm{tr}(X_\mu X_\mu^T X_\nu X_\nu^T), \quad \mathrm{tr}(X_{\mu\sigma} X_{\nu\sigma}^T X_{\rho\tau} X_{\mu\tau}^T X_{\nu\upsilon} X_{\rho\upsilon}^T) \tag{3.6}$$

The model exhibits $\mathrm{O}(N)^2 \times \mathrm{O}(D)^r$ symmetry, i.e. the action is invariant under the following two types of transformation of the matrices:

$$A_1, A_2 \in \mathrm{O}(N): \qquad X_{\mu_1\cdots\mu_r} \quad \to \quad A_1 X_{\mu_1\cdots\mu_r} A_2, \tag{3.7}$$

$$B_1, \ldots, B_r \in \mathrm{O}(D): \qquad X_{\mu_1\cdots\mu_r} \quad \to \quad (B_1)_{\mu_1\nu_1} \cdots (B_1)_{\mu_r\nu_r} X_{\nu_1\cdots\nu_r} \tag{3.8}$$

This model was introduced by Ferrari et al. in [4], but a simpler model with only one tensor index ($r = 1$) was introduced earlier by Ferrari in [3]. This simple model was based on a model studied by Carrozza and Tanasa in [2].

3.2 Degree and Scaling

Colored Graphs Representing Interaction Terms An interaction term $I_a(X)$ as in (3.5) can be represented by a colored graph $\mathcal{B}_a$ in the following way. By writing out the matrix multiplication and trace we get a product of $2k$ instances of $X_{\mu_1\cdots\mu_r ab}$ where the $r+2$ different indices are contracted pairwise. There are $2k$ vertices and $r+2$ colors in $\mathcal{B}_a$. Each vertex represents one of the $2k$ instances of $X_{\mu_1\cdots\mu_r ab}$. The colors $1, 2$ correspond to the two matrix indices a, b and the colors $2m \ldots, r+2$ correspond to the r tensor indices $\mu_1, \ldots, \mu_r$. Two vertices are connected by a color i if the corresponding indices of the two instances of $X_{\mu_1\cdots\mu_r ab}$ are contracted.

An example of the colored graphs corresponding to the first two interaction terms in 3.6 (called the *tetrahedral*, respectively *pillow*, interaction term) are given in Figure 3.1. Writing out the matrix multiplication and trace of these terms, we get:

$$\mathrm{tr}(X_\mu X_\nu^T X_\mu X_\nu^T) = X_{\mu ab} X_{\nu cb} X_{\mu cd} X_{\nu ad}, \tag{3.9}$$

$$\mathrm{tr}(X_\mu X_\mu^T X_\nu X_\nu^T) = X_{\mu ab} X_{\mu cb} X_{\nu cd} X_{\nu ad}, \tag{3.10}$$

for the tetrahedral, respectively pillow, interaction term. The two matrix indices are colors $1, 2$ (blue, red in the figure) and the single tensor index is color 3 (green in the figure). Examples of colored graphs corresponding to interaction terms in models with more than one tensor index can be found in Figure 4.4.

The graphs corresponding to interaction terms are bubbles, see Definition 2.5. Therefore, we will sometimes refer to these graphs as interaction bubbles.

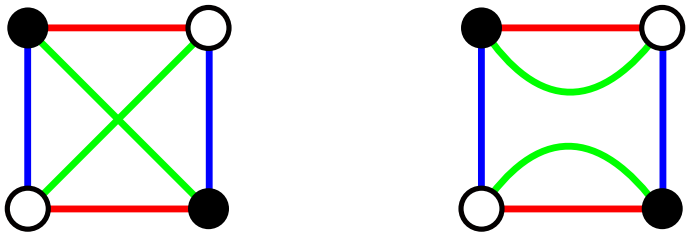

Figure 3.1: The tetrahedral interaction term (left) and pillow interaction term (right).

Degree When drawing the colored graph $\mathcal{B}_a$ corresponding to an interaction term there is a choice of the cyclic ordering of the $r+2$ colored edges around each vertex. There are $(r+1)!$ choices for this cyclic ordering. We will introduce the degree of an interaction vertex, which is associated with the different choices of cyclic ordering.

Fix a cyclic ordering $\sigma = (c_1 \cdots c_{r+2})$ of the $r+2$ colors and a partition P of the vertices of the graph into two sets: the vertices with counterclockwise ordering and the vertices with clockwise ordering. We define a rotation system on the graph by assigning the cyclic permutation σ to a counterclockwise ordered vertex and σ^{-1} to a clockwise ordered vertex. Also, we define a signature on the graph by assigning 1 to an edge when it connects two vertices of opposite ordering and -1 to an edge when it connects two vertices of the same ordering. The corresponding embedding of this graph is called a *jacket* and is denoted by $\mathcal{J}(\mathcal{B}_a, \sigma, P)$. When one draws the graph $\mathcal{B}_a$ one chooses a way to cyclically order the edges around each vertex, as we did in Figure 3.1. Here, the counterclockwise or clockwise ordering of each vertex was displayed as a filled or unfilled dot.

The jacket has a genus $g(\mathcal{J}(\mathcal{B}_a, \sigma, P))$. When we change the ordering of one of the vertices from counterclockwise to clockwise or vice versa, and at the same time change the sign of the edges incident on this vertex from 1 to -1 and from -1 to 1, we get a new jacket $\mathcal{J}(\mathcal{B}_a, \sigma, P')$. One can check that this does not change the genus. Hence, the genus of a jacket is independent of the partition P and we denote a jacket by $\mathcal{J}(\mathcal{B}_a, \sigma)$. Also, one checks that the genus of $\mathcal{J}(\mathcal{B}_a, \sigma^{-1})$ is the same as the genus of $\mathcal{J}(\mathcal{B}_a, \sigma)$. We now define the *degree* of $\mathcal{B}_a$ as follows:

$$\deg(\mathcal{B}_a) = \frac{1}{2} \sum_{\substack{\sigma \text{ cyclic} \\ \text{ordering}}} g(\mathcal{J}(\mathcal{B}_a, \sigma)). \tag{3.11}$$

The factor of $1/2$ takes into account that the jackets corresponding to σ and σ^{-1} have the same genus. Note that when $r = 1$, there are only three colors and hence two different cyclic orderings, which are each other's inverse. Therefore in this case, $\deg(\mathcal{B}_a)$ is equal to the unique genus of any embedding of $\mathcal{B}_a$.

Scaling of Coupling Constants We take the coupling constants τ_a associated with an interaction term $\mathcal{B}_a$ appearing in the action 3.4 to be dependent on D, but not N. This D dependence is as follows:

$$\tau_a = D^{\frac{2}{(r+1)!}\deg(\mathcal{B}_a)} \lambda_a, \tag{3.12}$$

where λ_a is independent of N, D. This defines the *scaling* of the coupling constants.

3.3 Free Energy Expansion and Large N, D Limit

Amplitude of Feynman Graphs A Feynman graph is a connected graph consisting of any number of copies of the interaction terms connected by propagators. More precisely, each vertex has one incident propagator, and this propagator is incident on a second vertex in either the same or a different interaction term. All possible ways of connecting copies of interaction terms by propagators such that the graph is connected give all possible Feynman graphs, although as we will see later a subset of these are selected by the large N, D limit. For notational convenience, we will consider propagators to be edges of color 0. Hence, since we have $r+2$ colors inside interaction terms, the number of colors in a Feynman graph is $r+3$. Note that Feynman graphs are bubbles, just like the copies of interaction terms contained in them.

Recall how a Feynman graph encodes the way the indices of the different copies of $X_{\mu_1\cdots\mu_r ab}$ involved are contracted. A Feynman graph represents a sum over all these contracted indices. Two vertices that are connected by an edge of color $1, \ldots, r$ correspond to two copies of $X_{\mu_1\cdots\mu_r ab}$ that have a contracted index. Also, two vertices that are connected by a propagator correspond to two copies of $X_{\mu_1\cdots\mu_r ab}$ that have *all* indices contracted. Therefore, it follows that all copies of $X_{\mu_1\cdots\mu_r ab}$ represented by vertices encountered on a $(0i)$-face ($i = 1, \ldots, r$; recall that a $(0i)$-face is a loop of alternating colors $0, i$) have the index corresponding to the color i contracted. Hence each (01)-face or (02)-face gives a factor of N and each $(0i)$-face for $i \geq 3$ gives a factor of D.

Furthermore, it follows from the action (3.4) and the scaling (3.12) that an interaction term $\mathcal{B}_a$ contributes a factor of $ND^{r+\frac{2}{(r+1)!}\deg(\mathcal{B}_a)}$, and each propagator a factor of $(ND^r)^{-1}$.

For a Feynman graph $\mathcal{B}$, denote by v, p, f, ϕ the number interaction bubbles (a.k.a. interaction terms) within $\mathcal{B}$, the number of propagators, the number of (01)-faces and (02)-faces, and the number of $(0i)$-faces for any $i \geq 3$, respectively. The total N, D dependence of $\mathcal{B}$ is then:

$$N^{v-p+f} D^{vr+\frac{2}{(r+1)!}\sum_{\mathcal{B}_a \text{ in } \mathcal{B}} \deg(\mathcal{B}_a) - pr + \phi} = N^{2-h} D^{r+h-\frac{\ell}{r+1}}, \tag{3.13}$$

where the numbers h, ℓ appearing on the right hand side are defined by this relation, and the sum is over all interaction bubbles $\mathcal{B}_a$ appearing in $\mathcal{B}$ (in particular repeated interaction terms are counted with multiplicity). The reason we have introduced h, ℓ in this way is because they have a convenient interpretation in terms of certain genera associated with $\mathcal{B}$, as we show next.

Interpretation of h It follows from (3.13) that:

$$h = 2 - v + p - f. \tag{3.14}$$

Consider $\mathcal{B}_{(012)}$ and an embedding where we use as faces all the (01)-, (02)- and (12)-faces. Denote by F_{ij} the number of (ij)-faces. Since each interaction bubble contributes precisely one (12)-face (representing the matrix trace) we have $F_{12} = v$. Also, because each vertex in $\mathcal{B}_{(012)}$ has precisely one incident edge of every color, there are $2p$ vertices and $3p$ edges. Euler's Formula (Theorem 2.7) then implies:

$$2 - 2g(\mathcal{B}_{(012)}) = 2p - 3p + F_{01} + F_{02} + F_{12} = -p + f + v. \tag{3.15}$$

Comparing this to (3.14) yields:

$$h = 2g(\mathcal{B}_{(012)}). \tag{3.16}$$

In particular, h is a non-negative integer.

Often one draws a less precise Feynman graph by replacing each interaction bubble by a single vertex with n incident propagators, where n is the number of vertices inside the interaction bubble. (Note that some of these n incident edges could have both ends attached to the same vertex, and in such case we count this edge with multiplicity two.) Topologically, this comes down to gluing a disk inside every (12)-face. Hence, it follows that the genus of this less precise Feynman diagram is equal to $g(\mathcal{B}_{(012)})$ and we will denote this specific genus from now on as g. Note that g is the genus of the Feynman graph when we "forget" the tensor indices, hence corresponds to the genus in matrix models.

Interpretation of ℓ For a Feynman graph $\mathcal{B}$ define the following expression, called the *index* of $\mathcal{B}$:

$$\mathrm{ind}_0(\mathcal{B}) = \sum_{1 \le i < j} \Big(g(\mathcal{B}_{(0ij)}) + F_{ij}(\mathcal{B}) - c(\mathcal{B}_{(0ij)}) - v + 1 \Big). \tag{3.17}$$

One can show that $F_{ij}(\mathcal{B}) - c(\mathcal{B}_{(0ij)}) - v + 1 \ge 0$ for all colors $i, j \ge 1$. Since the genus is also non-negative, we see that the index is non-negative. We will now show that $h = 2\,\mathrm{ind}_0(\mathcal{B})$. Other important properties of the index will become clear in the rest of this chapter.

First, we rewrite (3.17), using in the first step Euler's Formula, and in the second step the relation $3V(\mathcal{B}) = 2E(\mathcal{B}_{(0ij)})$:

$$\begin{aligned} 2\,\mathrm{ind}_0(\mathcal{B}) &= \sum_{1 \le i < j} (2c(\mathcal{B}_{(0ij)}) - V(\mathcal{B}) + E(\mathcal{B}_{(0ij)}) - F_{ij}(\mathcal{B}) - F_{0i}(\mathcal{B}) - F_{0j}(\mathcal{B}) \\ &\qquad + 2F_{ij}(\mathcal{B}) - 2c(\mathcal{B}_{(0ij)}) - 2v + 2) \\ &= \frac{(r+1)(r+2)}{2} \Big(\frac{1}{2} V(\mathcal{B}) - 2v + 2 \Big) + \sum_{1 \le i < j} F_{ij}(\mathcal{B}) \\ &\qquad - (r+1) \sum_{i=1}^{r+2} F_{0i}(\mathcal{B}) \end{aligned} \tag{3.18}$$

Next, we rewrite the definition of the degree (3.11) of an interaction term $\mathcal{B}_a$. Denote by F_σ the number of faces associated with the embedding with cyclic permutation $\sigma = (c_1 \cdots c_{r+2})$ of the $r+2$ colors. We see that:

$$F_\sigma = F_{c_1 c_2} + F_{c_2 c_3} + \ldots F_{c_{r+2} c_1}. \tag{3.19}$$

Observe that the term F_{ij} for some fixed i, j appears in F_σ for precisely $2r!$ different cyclic permutations σ. Also observe that the total number of cyclic permutations σ is $(r+1)!$. Using these two facts, the relation $(r+2)V(\mathcal{B}_a) = 2E(\mathcal{B}_a)$ and Euler's Formula, we find:

$$\begin{aligned} 2\deg(\mathcal{B}_a) &= \frac{1}{2} \sum_{\substack{\sigma \text{ cyclic} \\ \text{ordering}}} (2 - V(\mathcal{B}_a) + E(\mathcal{B}_a) - F_\sigma) \\ &= (r+1)! \left(1 + \frac{r}{4} V(\mathcal{B}_a)\right) - r! \sum_{1 \le i < j} F_{ij}(\mathcal{B}_a). \end{aligned} \tag{3.20}$$

Summing this equality over all v interaction bubbles in $\mathcal{B}$:

$$2 \sum_{\mathcal{B}_a \text{ in } \mathcal{B}} \deg(\mathcal{B}_a) = (r+1)! \left(v + \frac{r}{4} V(\mathcal{B})\right) - r! \sum_{1 \le i < j} F_{ij}(\mathcal{B}) \tag{3.21}$$

Then, we first deduce an expression for $\frac{\ell}{r+1}$ from (3.13), and in the second step we substitute the expression (3.14) for h and rewrite f, ϕ in terms of the F_{ij}. In the third step we use the relation $V(\mathcal{B}) = 2p$. This gives:

$$\begin{aligned} \frac{\ell}{r+1} &= r - vr + pr + h - \phi - \frac{2}{(r+1)!} \sum_{\mathcal{B}_a \text{ in } \mathcal{B}} \deg(\mathcal{B}_a) \\ &= r - vr + pr + 2 - v + p - \sum_{i=1}^{r+2} F_{0i}(\mathcal{B}) - v - \frac{r}{4} V(\mathcal{B}) + \frac{1}{r+1} \sum_{1 \le i < j} F_{ij}(\mathcal{B}) \\ &= \frac{r+2}{2} \left(\frac{1}{2} V(\mathcal{B}) - 2v + 2\right) - \sum_{i=1}^{r+2} F_{0i}(\mathcal{B}) + \frac{1}{r+1} \sum_{1 \le i < j} F_{ij}(\mathcal{B}) \end{aligned} \tag{3.22}$$

Comparing this with (3.18) we obtain:

$$\ell = 2 \operatorname{ind}_0(\mathcal{B}). \tag{3.23}$$

Free Energy Expansion and Large N, D Limit It follows from the above discussion that we can classify all Feynman graphs according to the non-negative integers $h, \ell \in \mathbb{N}_0$ associated with a Feynman graph. Furthermore, from the definition (3.17) of the index, the relation $h = 2g(\mathcal{B}_{(012)})$ and the fact that $F_{ij}(\mathcal{B}) - c(\mathcal{B}_{(0ij)}) - v + 1 \ge 0$ for all colors $i, j \ge 1$, it follows that:

$$h \le \ell. \tag{3.24}$$

Using this classification of the Feynman graphs, it follows from (3.13) that we can write the free energy as follows:

$$F = N^2 D^r \sum_{h, \ell \in \mathbb{N}_0} N^{-h} D^{h - \frac{\ell}{r+1}} F_{h,\ell}, \tag{3.25}$$

where $F_{h,\ell}$ is independent of N, D and represents the contribution of all Feynman graphs with fixed h, ℓ.

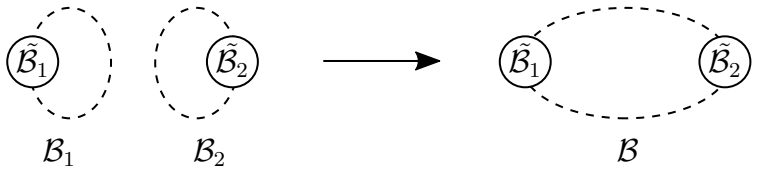

Figure 3.2: The insertion of two Feynman graphs $\mathcal{B}_1, \mathcal{B}_2$ into each other to obtain a new graph $\mathcal{B}$. The dashed lines represent propagators.

Now we want to take the limit $N, D \to \infty$ of the expression $F/(N^2 D^r)$ and see which Feynman graphs are selected. Notice that the power of D in the factor $D^{h-\frac{\ell}{r+1}}$ becomes positive when h is sufficiently close to ℓ. Hence, if we first take the limit $D \to \infty$ the free energy will diverge. Therefore, the large N, D limits do not commute and we first have to take the large N limit and then the large D limit. First taking $N \to \infty$ selects all Feynman graphs with $h = 0$. Then, taking $D \to \infty$ gives the extra condition $\ell = 0$.

Since $h \leq \ell$ and $\ell = 2\,\mathrm{ind}_0(\mathcal{B})$, the conditions $h = \ell = 0$ for a Feynman graph $\mathcal{B}$ are equivalent to $\mathrm{ind}_0(\mathcal{B}) = 0$. Solving this equation for a specific choice of interaction terms will be the subject of the next chapter. We will call the Feynman graphs $\mathcal{B}$ satisfying $\mathrm{ind}_0(\mathcal{B}) = 0$ *lowest order* (LO) Feynman graphs.

3.4 Feynman Graph Insertion and MST Interactions

Inserting Feynman Graphs into Each Other Given two Feynman graphs $\mathcal{B}_1$ and $\mathcal{B}_2$, we can create a new graph $\mathcal{B}$ by the following procedure: select one propagator in $\mathcal{B}_1$ and one in $\mathcal{B}_2$ and cut them open to obtain the so-called *two-point graphs* $\tilde{\mathcal{B}}_1, \tilde{\mathcal{B}}_2$. Then, attach one end of the cut propagator in $\tilde{\mathcal{B}}_1$ to one end of the cut propagator in $\tilde{\mathcal{B}}_2$, and do the same for the remaining two ends. This process is called *insertion* and is pictured in Figure 3.2. Note that in general there are multiple ways to insert two Feynman graphs into each other, since there is a choice in the propagators to be cut open and there are also two ways to attach these cut propagators to each other.

A very convenient property of the index is that the index of the new graph $\mathcal{B}$ is the sum of the indices of $\mathcal{B}_1, \mathcal{B}_2$. This is the content of the following Proposition. This is Proposition 2.5 in [4] and a proof can be found there.

Proposition 3.1. *Let $\mathcal{B}_1, \mathcal{B}_2$ be two Feynman graphs and $\mathcal{B}$ the graph obtained after insertion of $\mathcal{B}_1, \mathcal{B}_2$ into each other. Then:*

$$\mathrm{ind}_0(\mathcal{B}) = \mathrm{ind}_0(\mathcal{B}_1) + \mathrm{ind}_0(\mathcal{B}_2). \tag{3.26}$$

A useful consequence of this Proposition is that if we can find just one LO Feynman graph $\mathcal{B}$ (i.e. $\mathrm{ind}_0(\mathcal{B}) = 0$), then we can generate an infinite family of LO Feynman graphs using $\mathcal{B}$: First we can insert two copies of $\mathcal{B}$ into each other and the resulting graph will still have index equal to zero (this insertion can in general be done in multiple ways). Then, we can repeatedly insert copies of $\mathcal{B}$ into this graph to obtain an infinite number of index zero graphs.

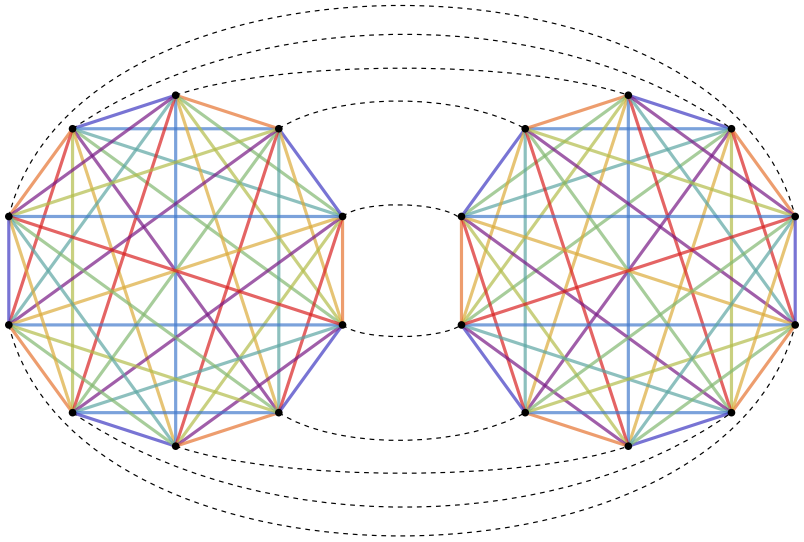

Figure 3.3: Example of an elementary mirror melon. The interaction term used here is the unique (up to isomorphism) MST coloring of the complete graph with 10 vertices. Two copies of this graph, mirrored images of each other, are connected by propagators.

MST Interaction Terms We will consider the following type of interaction term, which has some interesting properties and will play an important role in the next chapter.

Definition 3.2. An interaction term is *maximally single trace* (MST) if for any pair of distinct colors i, j there is only one (ij)-face.

In other words, for every pair of distinct colors i, j, there is an (ij)-face that visits *all* the vertices in the interaction term. This type of interaction term was introduced in [4]. We have already seen an example of an MST interaction term: the tetrahedral interaction term is MST, but the pillow interaction term is not. Examples of MST interactions with 10 and 16 vertices are shown in Figure 4.4.

If we include only MST interaction terms, the expression for the index of a Feynman graph $\mathcal{B}$ becomes very simple. Since for every pair of colors i, j we have $F_{ij}(\mathcal{B}) = v$ (one (ij)-face for each of the v interaction bubbles inside $\mathcal{B}$) and $c(\mathcal{B}_{(0ij)}) = 1$ (the (ij)-face in an interaction bubble visits every vertex in the bubble, hence $\mathcal{B}_{(0ij)}$ remains connected) (3.17) gives:

$$\mathrm{ind}_0(\mathcal{B}) = \sum_{1 \le i < j} g(\mathcal{B}_{(0ij)}). \tag{3.27}$$

Let $\mathcal{B}_{\mathrm{MST}}$ be an MST interaction term. The *elementary mirror melon* associated with $\mathcal{B}_{\mathrm{MST}}$ is the Feynman graph $\mathcal{B}_{\mathrm{mirror}}$ consisting of two copies of $\mathcal{B}_{\mathrm{MST}}$, where each vertex in one copy is attached via a propagator to the equivalent vertex in the other copy. See Figure 3.3 for an example.

It turns out that $\mathcal{B}_{\mathrm{mirror}}$ is a LO Feynman graph. To see this, we substitute the two equations below in (3.18) to find $\mathrm{ind}_0(\mathcal{B}_{\mathrm{mirror}}) = 0$. For the first equation below,

note that there are precisely two (ij)-faces in $\mathcal{B}_{\text{mirror}}$ for every pair of colors i, j (one in each copy of $\mathcal{B}_{\text{MST}}$), and that there are $\frac{(i+1)(i+2)}{2}$ possibilities for the pairs of colors i, j. For the second equation below, note that each $(0i)$-face corresponds to one edge of color i in each copy of $\mathcal{B}_{\text{MST}}$, hence $\sum_{i=1}^{r+2} F_{0i}(\mathcal{B}_{\text{mirror}})$ is the number of edges in $\mathcal{B}_{\text{MST}}$. Also, $2E(\mathcal{B}_{\text{MST}}) = (r+2)V(\mathcal{B}_{\text{MST}})$ and $V(\mathcal{B}_{\text{MST}}) = \frac{1}{2}V(\mathcal{B}_{\text{mirror}})$.

$$\sum_{1\leq i<j} F_{ij}(\mathcal{B}_{\text{mirror}}) = (r+1)(r+2) \tag{3.28}$$

$$\sum_{i=1}^{r+2} F_{0i}(\mathcal{B}_{\text{mirror}}) = \frac{r+2}{4} V(\mathcal{B}_{\text{mirror}}) \tag{3.29}$$

One can also show the reverse implication: if the elementary mirror melon corresponding to an interaction term is LO, then the interaction term must be MST. We refer to

Now that we know that $\mathcal{B}_{\text{mirror}}$ is LO, we can generate an infinite family of graphs by starting with $\mathcal{B}_{\text{mirror}}$ and repeatedly inserting new copies of $\mathcal{B}_{\text{mirror}}$. We call the graphs obtained in this way *melonic*. All melonic graphs are LO Feynman graphs, but it is not clear if they constitute all of the LO graphs: there could be LO graphs that are not obtained by this process of repeated insertion of $\mathcal{B}_{\text{mirror}}$. In the next chapter, we introduce a certain class of MST interaction terms for which we can prove that the melonic graphs are all the LO Feynman graphs.

Optimal Scaling Why would we want to use the scaling (3.12) and not something else? The following proposition partly answers this question.

Proposition 3.3. *If an interaction term $\mathcal{B}_a$ appears in some LO Feynman graph, then the scaling corresponding to $\mathcal{B}_a$ is optimal in the following sense: raising or lowering the power of D in the scaling* (3.12) *would result in a theory where $\mathcal{B}_a$ can never appear in a LO graph.*

Proof. Consider a LO graph $\mathcal{B}$ containing $\mathcal{B}_a$. We can create an infinite family of LO graphs by starting with $\mathcal{B}$ and repeatedly inserting copies of $\mathcal{B}$ onto propagators. Hence we get LO graphs containing arbitrarily many of copies of $\mathcal{B}_a$. For the scaling (3.12) the powers of D in such leading order graphs exactly cancel. If we would raise the power of D in the scaling, then the infinite family of graphs generated by $\mathcal{B}$ would contribute terms to the free energy scaling with arbitrarily high powers of D. Hence in the $D \to \infty$ limit the free energy diverges. If we would lower the power of D in scaling, $\mathcal{B}$ would no longer be leading order. □

Since MST interaction terms always appears in some LO Feynman graph (the elementary mirror melon associated with an MST interaction is always LO), we deduce from this Proposition that the scaling (3.12) is optimal for at least all the MST interactions.

4 MST Colorings of Complete Graphs and Melonic Feynman Graphs

In this chapter we will show that a theory using an MST coloring of a complete graph as the interaction term, yields melonic LO Feynman graphs. Recall that the complete graph K_n is the graph with n vertices where each vertex is adjacent to every other vertex. Note that the fact that each vertex should have precisely one edge of every color incident on it requires that the number of colors $r + 2$ equals $n - 1$. As we saw in the previous chapter, after performing the large N and D limits we obtain all Feynman graphs whose parameters satisfy $h = \ell = 0$. In the following we will call such graphs lowest order (LO) Feynman graphs.

Recall that, by definition, an interaction term is MST if for all distinct colors i, j there is a unique (ij)-face (cycle of alternating colors i, j). As a consequence, the (ij)-face visits every vertex in the graph. Also, recall that an interaction term is MST if and only if its corresponding elementary mirror melon is a LO Feynman graph. One can generate an infinite family of Feynman graphs by beginning with the propagator loop and repeatedly inserting an elementary mirror melon onto a propagator. Graphs that can be obtained in this way are called melonic. A melonic graph is also a LO Feynman graph, but the converse is not necessarily true. Showing that this *is* true for an MST coloring of a complete graph is the main result of this chapter:

Theorem 4.1. *If the interaction term is a maximally single trace coloring of a complete graph, then all lowest order Feynman graphs are melonic.*

The proof of this theorem will be given in Section 4.2. We will rely on an important property, the so-called odd-even property, which we show is satisfied by an MST coloring of a complete graph in Section 4.1. Section 4.3 contains background information about MST colorings of a complete graph.

Theorem 4.1 implies that we can completely describe all LO Feynman graphs in the theory, and the description is simple: the LO Feynman graphs are precisely all the graphs that one can create by repeated insertions of the elementary mirror melon.

In a paper by Ferrari et al. [4] a certain coloring of the complete graph K_{p+1} was defined. It was shown that this interaction term is MST if and only if p is an odd prime. Furthermore, it was shown that when using this interaction term all LO Feynman graphs are melonic. The strategy used to prove Theorem 4.1 in Section 4.2 is based on Section 4 in [4], but adapted to use the odd-even property and thereby proving a more general result.

4.1 The Odd-Even Property

We introduce the odd-even property and show that any MST coloring of the complete graph K_n for even $n \geq 6$ satisfies this property.

Definition 4.2. Let $\mathcal{B}$ be a colored graph. We will say that an edge v_1v_2 is *indexed at length* $n \in \mathbb{Z}_{\geq 1}$ *by* two distinct colors i, j if there exists a path of length n (i.e. n edges in the path) between v_1 and v_2 with edges of alternating colors i, j. We will say that $\mathcal{B}$ satisfies the *odd-even* property if the following holds: for any two distinct edges v_1v_2 and w_1w_2 with the same color k there exist distinct colors i, j, both unequal to k, such that v_1v_2 is indexed at an even length by i, j and w_1w_2 is indexed at an odd length by i, j, or vice versa.

Theorem 4.3. *Let $\mathcal{K}_n$ be a maximally single trace coloring of the complete graph K_n for even $n \geq 6$. Then $\mathcal{K}_n$ satisfies the odd-even property.*

Proof. In the following we will often implicitly use that every vertex in $\mathcal{K}_n$ is incident on every other vertex, and that every color occurs exactly once among the edges of any vertex.

Let v_1v_2, w_1w_2 be distinct edges with the same color k. See (a) in Figure 4.1. Let $j \neq k$ be the color of the edge v_1w_1, and z the vertex incident on v_2 via the edge of color j. Note that $z \neq w_2$, else the (kj)-face $v_1v_2w_2w_1v_1$ does not visit all ≥ 6 vertices in $\mathcal{K}_n$, contradicting the MST property (see (b) in the figure). Let $i \neq j$ be the color of the edge zw_2.

Consider the (ij)-face, which visits all vertices by the MST property. Starting with the edge of color i incident on vertex v_1, this face visits the vertices z, w_1, w_2, v_2 in some order before returning to v_1 and we treat four separate cases depending on which vertex is visited *first*. The number of each case corresponds to one of the numbered insets in the figure.

1. First z: This is impossible since z already has edges of color i, j incident on w_2, respectively v_2.
2. First w_1: This is impossible since the (ij)-face does not visit v_2, w_2, z.
3. First w_2: Notice that there is a path of alternating colors i, j from v_1 starting with an edge of color i and ending at v_2 with an edge of color j. Hence this path has even length and therefore v_1v_2 is indexed at even length by i, j. There is a path of alternating colors i, j starting at w_1 with color j and ending at w_2 with color j. Hence w_1w_2 is indexed at odd length by i, j.

4. First v_2: Similarly as in the previous case, we now see that v_1v_2 is indexed at odd length by i, j and w_1w_2 is indexed at even length.

We conclude that $\mathcal{K}_n$ satisfies the odd-even property. □

Distinguishable Edges and Vertices The odd-even property implies that we can always distinguish between two edges of the same color. Indeed, one of the edges is indexed at odd length by a pair of colors i, j and the other edge is indexed at even length by i, j, which gives a way to distinguish the edges.

The same is true for two vertices v_1, v_2. To see this, let k be the color of the edge v_1v_2 and choose any color $i \neq k$. Then, consider the two distinct edges of color i that are adjacent to v_1 and v_2. These edges can be distinguished from one another, hence also the vertices v_1, v_2. Intuitively, the odd-even property implies that the interaction term has very little symmetry. Section 4.3 contains more information about MST colorings of a complete graph.

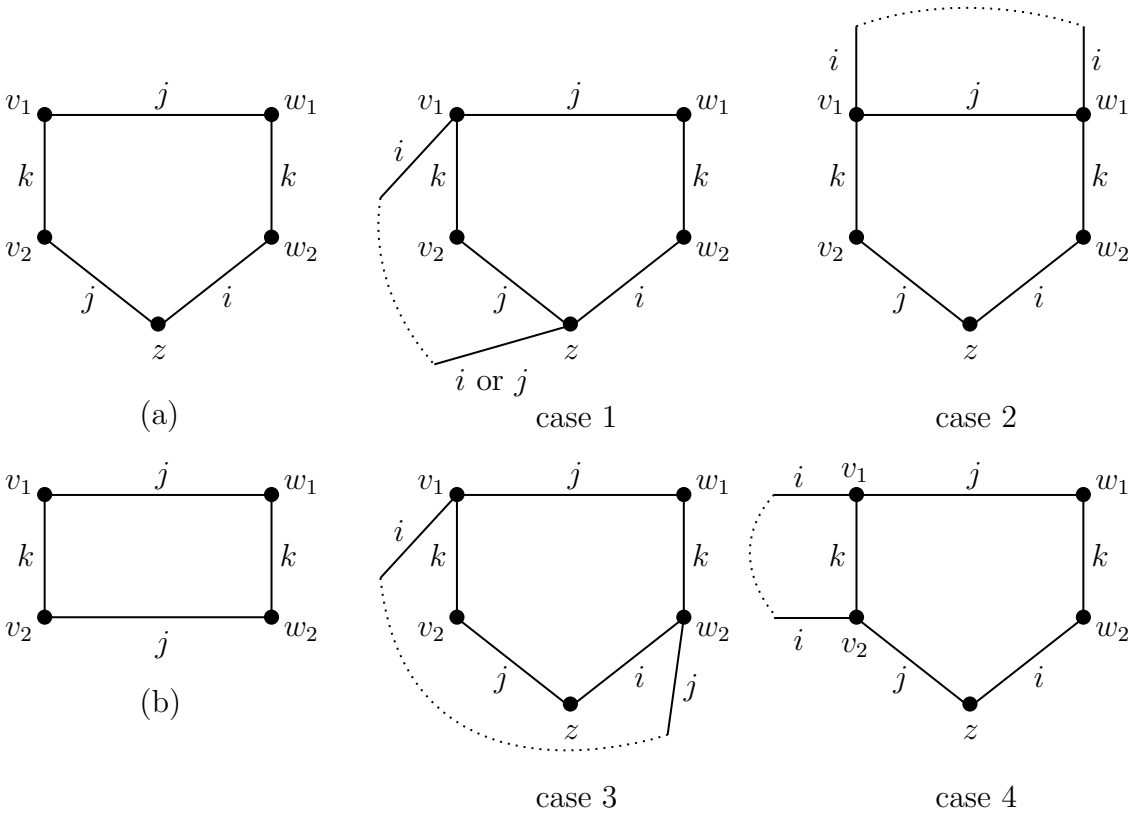

Figure 4.1: See the proof of Theorem 4.3. Note that not the entire graph is shown, only the parts that are relevant for the proof. The dotted lines represent paths of alternating colors i, j and do not visit any of the vertices displayed as a dot.

4.2 Structure of LO Feynman Graphs

In this section, $\mathcal{B}$ will denote a LO Feynman graph in a theory with an interaction term equal to any MST coloring $\mathcal{K}_n$ of the complete graph with n vertices, where $n \geq 4$ is even. We will prove a number of properties of $\mathcal{B}$, leading to a description of the general structure of $\mathcal{B}$ in Proposition 4.9. The odd-even property will play a role in the proofs. Finally, we use Proposition 4.9 to prove Theorem 4.1. The proof strategy of this section is based on Section 4 in [4], adapted to our more general setting.

The LO Feynman graphs are precisely those graphs $\mathcal{B}$ that satisfy $\mathrm{ind}_0(\mathcal{B}) = 0$. By (3.27), this is equivalent to:

$$g(\mathcal{B}_{(0ij)}) = 0 \quad \text{for all colors } i, j. \tag{4.1}$$

We can derive an equivalent condition as follows. Note that:

$$\sum_{1 \leq i < j} F_{ij}(\mathcal{B}) = \frac{(r+1)(r+2)}{2} v, \tag{4.2}$$

since there is one (ij)-face for each of the v interaction bubbles in $\mathcal{B}$, and $\frac{(r+1)(r+2)}{2}$ pairs of colors i, j. Using this equation, and the fact that $r + 2 = n - 1$ and $V(\mathcal{B}) = nv$, (3.18) and $\mathrm{ind}_0(\mathcal{B}) = 0$ give the following condition:

$$\sum_i F_{0i} = \frac{1}{4}(n-1)(n-2)v + n - 1, \tag{4.3}$$

which is equivalent to (4.1).

Condition (4.1) means that the graph consisting of only the propagators and the edges of any two distinct colors is planar. We will use this fact in relation to the following lemma:

Lemma 4.4. *A planar 3-bubble cannot have cycles of odd length.*

Proof. Note that there are precisely two cyclic orderings of three colors. The planar embedding of the 3-bubble corresponds to a rotation system, i.e. each vertex is assigned one of the two cyclic orderings of the three colored edges. By our definition of the genus, the faces of the embedding are all the possible cycles of two distinct alternating colors. Thus, the fact that the embedding is planar implies that two vertices connected by an edge must have opposite cyclic orderings assigned to them. This induces a partition of the vertices in two sets that makes the graph bipartite. It is clear that a bipartite graph cannot have cycles of odd length, concluding the proof. □

The following two lemmas give information about how the interaction bubbles within $\mathcal{B}$ can be connected by propagators.

Lemma 4.5. *In a $(0i)$-face in $\mathcal{B}$ for any color i, two distinct edges of color i lie in two distinct interaction bubbles.*

Proof. Consider the following $(0i)$-face:

$$v_1 \overset{i}{-} v_2 \overset{0}{-} \cdots \overset{0}{-} v_{2k+1} \overset{i}{-} v_{2k} \overset{0}{-} \cdots \overset{0}{-} v_1, \tag{4.4}$$

where $v_1v_2, v_{2k+1}v_{2k}$ are two distinct edges of color i in the same interaction bubble. Then v_{2k+1} and v_1 are connected by an edge of color $j \neq i$. Then the cycle:

$$v_1 \overset{i}{-} v_2 \overset{0}{-} \cdots \overset{0}{-} v_{2k+1} \overset{j}{-} v_1 \tag{4.5}$$

lies in $\mathcal{B}_{(0ij)}$ and has odd length. This contradicts Lemma 4.4 applied to $\mathcal{B}_{(0ij)}$, which is planar according to (4.1). □

Lemma 4.6. *Two distinct vertices in the same interaction bubble in $\mathcal{B}$ cannot be connected by a propagator.*

Proof. Assume v_1, v_2 are two distinct vertices in the same interaction bubble and are connected by a propagator. Let v_3 be any other vertex within the same interaction bubble, and let i, j be the (distinct) colors of the edges v_1v_3, respectively v_2v_3. Then:

$$v_1 \overset{i}{-} v_3 \overset{j}{-} v_2 \overset{0}{-} v_1, \tag{4.6}$$

has odd length in $\mathcal{B}_{(0ij)}$, contradicting (4.1) and Lemma 4.4. □

Denote by F_k the number of $(0i)$-faces of length $2k$ in $\mathcal{B}$ for any color i. Note that there are no $(0i)$-faces of odd length, since otherwise some vertex will have two distinct edges of the same color. The following lemma implies that there exists a $(0i)$-face for some color i of length four, which we will use later.

Lemma 4.7. *We have $F_2 \geq \frac{1}{2}n(n-1)$.*

Proof. Any $(0i)$-face of length $2k$ passes through k propagators. Also, each propagator lies in $n-1$ different $(0i)$-faces, one for each of the $n-1$ colors i. This implies:

$$\sum_{k=1}^{\infty} kF_k = (n-1)p, \tag{4.7}$$

where p is the number of propagators. There are v interaction bubbles, hence vn vertices. Each vertex has one propagator attached, hence $2p = vn$. Thus the above equation becomes:

$$\sum_{k=1}^{\infty} kF_k = \frac{1}{2}vn(n-1). \tag{4.8}$$

Notice that:

$$\sum_i F_{0i} = \sum_{k=1}^{\infty} F_k. \tag{4.9}$$

It follows from Lemma 4.6 that $F_1 = 0$, hence we see:

$$\frac{n}{2}\sum_{k=1}^{\infty} F_k - \frac{n-2}{4}\sum_{k=1}^{\infty} kF_k = F_2 + \frac{1}{4}\sum_{k=3}^{\infty} \left[2n - (n-2)k\right] F_k. \tag{4.10}$$

Using the identity (4.9) in (4.3), we can substitute (4.3) and (4.8) into the left hand side of the equality above, which yields $\frac{1}{2}n(n-1)$. Then the equality above gives:

$$F_2 = \frac{1}{2}n(n-1) + \frac{1}{4}\sum_{k=3}^{\infty}\left[-2n + (n-2)k\right]F_k. \tag{4.11}$$

When $n \geq 6$, we have $-2n + (n-2)k \geq 0$ for $k \geq 3$, which finishes the proof in these cases.

For $n = 4$, we show that $F_3 = 0$. Since $-2n + (n-2)k = -8 + 2k \geq 0$ for $k \geq 4$, this finishes the proof for this case. Assume that $F_3 > 0$, i.e. there exists a $(0i)$-face of length 6. We may assume $i = 1$ since the other cases are similar:

$$v_1^1 \overset{1}{-} v_2^1 \overset{0}{-} v_1^2 \overset{1}{-} v_2^2 \overset{0}{-} v_1^3 \overset{1}{-} v_2^3 \overset{0}{-} v_1^1. \tag{4.12}$$

By Lemma 4.5 the three edges of color 1 lie in three distinct interaction bubbles. For each of these edges $v_1^i v_2^i$ we can find a third vertex w^i such that $v_1^i w^i$ has color 2 and $v_2^i w^i$ has color 3. Here we used the fact that we know exactly which interaction bubble we are dealing with: the MST interaction on K_4 is unique, it is the tetrahedral interaction. Then we have a cycle of odd length in $\mathcal{B}_{(023)}$:

$$v_1^1 \overset{2}{-} w^1 \overset{3}{-} v_2^1 \overset{0}{-} v_1^2 \overset{2}{-} w^2 \overset{3}{-} v_2^2 \overset{0}{-} v_1^3 \overset{2}{-} w^3 \overset{3}{-} v_2^3 \overset{0}{-} v_1^1, \tag{4.13}$$

contradicting (4.1) and Lemma 4.4. □

Let v, w be two vertices in $\mathcal{B}$ lying in two distinct interaction bubbles. We say that v and w are *equivalent* if they correspond to the same vertex in $\mathcal{K}_n$. Also, we say that two edges v_1v_2 and w_1w_2 in $\mathcal{B}$, lying in two distinct interaction bubbles, are *equivalent* if they correspond to the same edge in $\mathcal{K}_n$. Recall the discussion at the end of Section 4.1 about the fact that the vertices, as well as the edges, in $\mathcal{K}_n$ can be distinguished from one another by the structure of the faces.

We are now ready to prove the following lemma, which tells us exactly what a $(0k)$-face of length 4 looks like. This is where the odd-even property, which our interaction term satisfies by Theorem 4.3, comes into play.

Lemma 4.8. *Let*

$$v_1 \overset{k}{-} v_2 \overset{0}{-} w_2 \overset{k}{-} w_1 \overset{0}{-} v_1 \tag{4.14}$$

be a $(0k)$-face of length 4 for any color $k \neq 0$. Then v_1 and w_1 are equivalent, and v_2 and w_2 are equivalent.

Proof. By Lemma 4.5 the edges v_1v_2 and w_1w_2 lie in two distinct interaction bubbles. Assume that these two edges are not equivalent. The odd-even property (Theorem 4.3) implies that there exist distinct colors i, j such that v_1v_2 is indexed at even length and w_1w_2 is indexed at odd length, or vice versa. This gives us the following cycle: first a path of alternating colors i, j from v_1 to v_2, then an edge of color 0, then a path of alternating colors i, j from w_2 to w_1 and finally back to v_1 via an

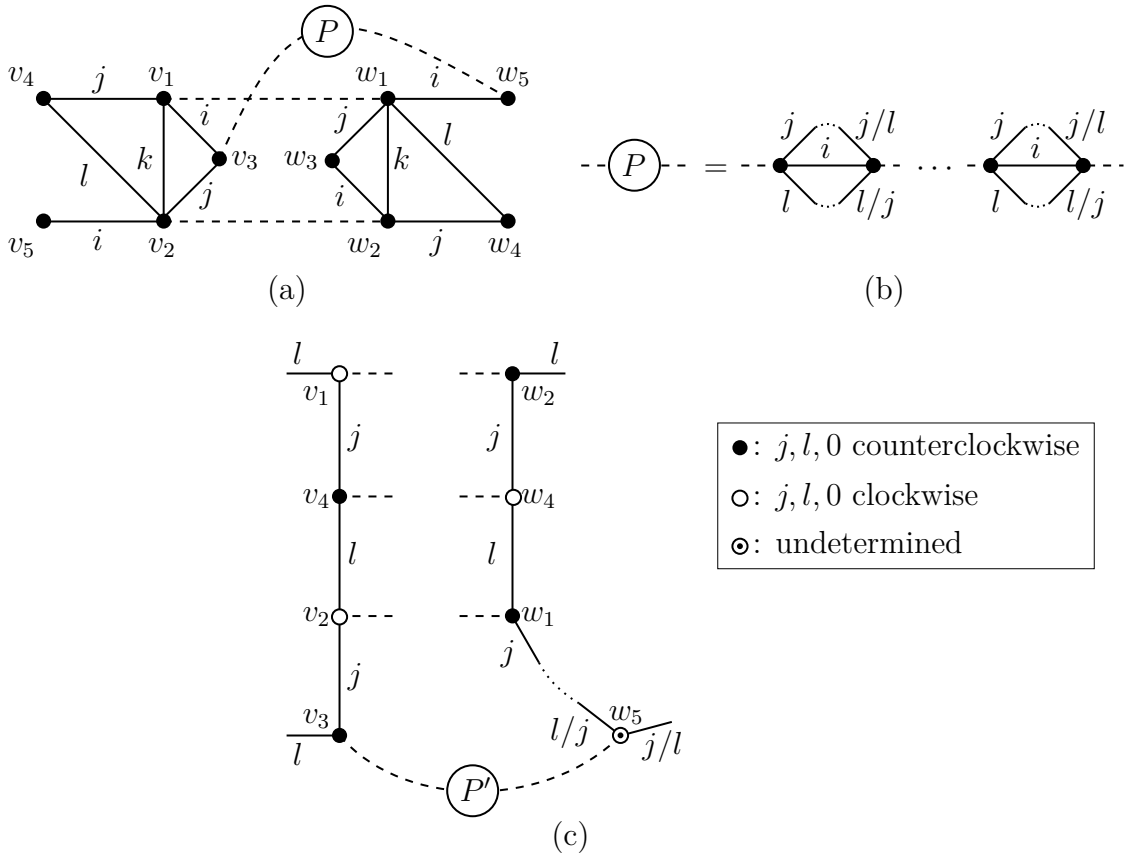

Figure 4.2: See the proof of Lemma 4.8. Dashed lines are propagators. Edges labeled j/l or l/j can have either color, depending on the precise structure. (a): The vertices v_1, v_2, w_1, w_2 lie in a $(0i)$-face of length four, and v_1, w_2 are equivalent and v_2, w_1 are equivalent. This structure is shown to be impossible. P consists of the section of the $(0i)$-face between v_3 and w_5 together with the (jl)-faces inside every interaction bubble that it visits. (b): P together with the (distinct) (jl)-faces in every visited interaction bubble. P can visit any number of interaction bubbles (not just two as shown here). (c): A planar embedding of $\mathcal{B}_{(0jl)}$. The vertices are shown as (un)filled dots depending on the choice of cyclic ordering of the incident edges. Only part of the graph $\mathcal{B}_{(0jl)}$ is drawn. P' is P as in (b), but with the edges of color i deleted. One checks that it is impossible to connect v_1, w_1 and to connect v_2, w_2 by propagators without intersecting edges, leading to a contradiction.

edge of color 0. This cycle has odd length and consists only of edges of colors $0, i, j$, contradicting (4.1) and Lemma 4.4. Hence v_1v_2 and w_1w_2 are equivalent edges.

Therefore, either v_1, w_1 are equivalent and v_2, w_2 are equivalent, or v_1, w_2 are equivalent and v_2, w_1 are equivalent. Assume the latter. We show that this leads to a contradiction, thereby finishing the proof. Choose a vertex v_3 inside the same interaction bubble as v_1 and v_2, but not equal to v_1 or v_2. See Figure 4.2 (a). Vertex v_3 corresponds to the (unique) equivalent vertex w_3 inside the interaction bubble that w_1 and w_2 belong to. Let i be the color of the edge v_1v_3. Since v_1 and w_2 are equivalent, the edge w_2w_3 is equivalent to v_1v_3 and therefore also has color i. Similarly, v_2v_3 and w_1w_3 have the same color, say j. Let v_4, respectively w_4, be the vertex adjacent to v_1, respectively w_2, via the edge of color j. Let v_5, respectively w_5, be the vertex adjacent to v_2, respectively w_1, via the edge of color i. Finally, let l be the color of the equivalent edges v_2v_4 and w_1w_4.

Consider the $(0i)$-face passing through w_5, w_1, v_1, v_3. Let P be the remaining part of this $(0i)$-face between v_3 and w_5. Note that by Lemma 4.5 the vertices appearing in P do not lie in the two interaction bubbles where v_1, v_2, w_1, w_2 lie in, and therefore no edges in P are the same as the ones already pictured in inset (a). Also by this lemma, each edge of color i within P lies in a different interaction bubble. In inset (b) we show the (unique) (j, l)-face in each of these interaction bubbles.

Next, consider $\mathcal{B}_{(0jl)}$. According to (4.1) this graph is planar. As explained in the proof of Lemma 4.4, since the graph is a planar 3-bubble, the graph is bipartite: one type of vertices has the cyclic ordering $0, j, l$ going counterclockwise for the three adjacent colored edges and the other type of vertices has the cyclic ordering $0, j, l$ going clockwise. Drawing the vertices and edges on a plane and respecting this cyclic ordering yields an embedding where no edges intersect.

In inset (c) $\mathcal{B}_{(0jl)}$ has been drawn, but some vertices and edges have been left out. Clearly, after removing edges and vertices the resulting graph still has no overlapping edges. Without loss of generality, we have made a choice in the cyclic ordering of the incident edges of a vertex. The path P' is P as in inset (b), but without the edges of color i. The vertices v_1 and w_1, as well as the vertices v_2 and w_2, should be connected by an edge of color 0. One easily sees that this is impossible without having intersecting edges. This yields the desired contradiction. □

Define a *two-point Feynman graph* to be a Feynman graph with one of the propagators cut open. Note that the simplest two-point Feynman graph is just one propagator. The following proposition gives the general structure of $\mathcal{B}$.

Proposition 4.9. *$\mathcal{B}$ contains n two-point LO Feynman graphs and two distinct interaction bubbles such that each of the two-point LO Feynman graphs is connected to two equivalent vertices of the two interaction bubbles. Furthermore, the two-point LO Feynman graphs are pairwise disjoint and at least two of them are equal to the propagator. See Figure 4.3 (a).*

Proof. By Lemma 4.7 there exists a $(0k)$-face for some color k:

$$v_1 \overset{k}{-} v_2 \overset{0}{-} w_2 \overset{k}{-} w_1 \overset{0}{-} v_1, \tag{4.15}$$

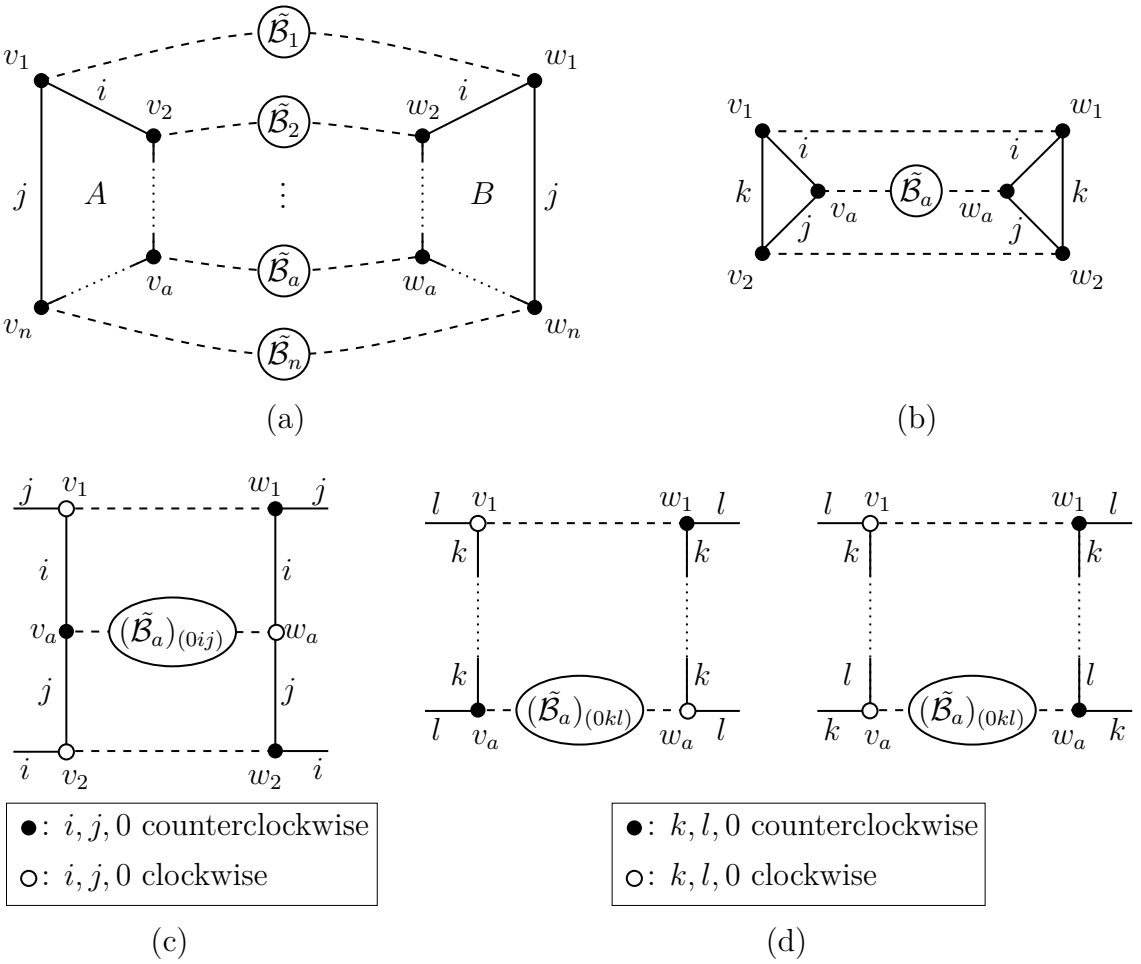

Figure 4.3: Inset (a) depicts the structure of any LO Feynman graph. Dashed lines are propagators and dotted lines are part of a face. There are two distinct interaction bubbles A, B and n pairwise disjoint two-point LO Feynman graphs $\tilde{\mathcal{B}}_a$, such that each $\tilde{\mathcal{B}}_a$ is connected via propagators to a vertex v_a in A and the equivalent vertex w_a in B. At least two of the $\tilde{\mathcal{B}}_a$ are equal to just the propagator. Note that in this figure only the (ij)-faces of A, B are shown for simplicity and the structure of the graph is the same for any choice of colors i, j. The other insets aid in the proof of Proposition 4.9.

and by Lemma 4.8 we know that v_1 and w_1 are equivalent, and v_2 and w_2 are equivalent. Let A, respectively B, be the interaction bubble containing v_1, v_2, respectively the interaction bubble containing w_1, w_2. A, B are the two distinct interaction bubbles mentioned in the statement of the Lemma. Let v_a be any vertex other than v_1, v_2 in A and let w_a be the corresponding equivalent vertex in B. See Figure 4.3 (b). Let i be the color of the equivalent edges v_1v_a, w_1w_a and j the color of the equivalent edges v_2v_a, w_2w_a. In order to complete the $(0i)$-face passing through v_a, v_1, w_1, w_a the vertices v_a, w_a must be connected via the remaining part of the $(0i)$-face, which is a path P. Let $\tilde{\mathcal{B}}_a$ be the subgraph of $\mathcal{B}$ consisting of P together with all edges and vertices in $\mathcal{B}$ connected to P via a path that does not pass through v_a or w_a.

According to (4.1) the 3-bubble $\mathcal{B}_{(0ij)}$ is planar. Hence the graph is bipartite and can be drawn on a plane, with one type of vertices having the cyclic ordering $0, i, j$ going counterclockwise for the three adjacent colored edges and the other type of vertices having the cyclic ordering $0, i, j$ going clockwise, with no edges intersecting. In inset (c) we draw a part of $\mathcal{B}_{(0ij)}$ using this embedding. Note that we can also switch the cyclic ordering of all the vertices, but the figure will be similar. We deduce that $(\tilde{\mathcal{B}}_a)_{(0ij)}$ does not contain any edges or vertices from the interaction bubbles A or B, since otherwise an edge in $(\tilde{\mathcal{B}}_a)_{(0ij)}$ would intersect an edge in the cycle $v_1, v_a, v_2, w_2, w_a, w_1, v_1$. Note that since the interaction bubbles are MST vertices are connected via a path in $\mathcal{B}_{(0ij)}$ if and only if they are connected via a path in $\mathcal{B}$. Hence, we find that $\tilde{\mathcal{B}}_a$ is not connected to A or B via propagators except the propagators adjacent to v_a and w_a.

Since we choose v_a to be any vertex in A other than v_1, v_2, we can repeat the argument above for all the remaining vertices in A to get the subgraphs $\tilde{\mathcal{B}}_a$ connected to the equivalent vertices v_a, w_a and not to any other vertices in A or B. Since v_1, w_1 and v_2, w_2 are both directly connected via a propagator, we can set the corresponding $\tilde{\mathcal{B}}_1, \tilde{\mathcal{B}}_2$ to be equal to the propagator. Then we get the structure as in inset (a). Note that in this figure the colors i, j and the labeling of the vertices is not necessarily the same as in the proof above.

Observe that if any two $\tilde{\mathcal{B}}_a, \tilde{\mathcal{B}}_b$ are not disjoint, then they would be connected via propagators to A and B in two different ways: via v_a and w_a and also via v_b and w_b. But we showed that they are only connected via propagators to A and B in one way. Hence the $\tilde{\mathcal{B}}_a$ are pairwise disjoint.

It remains to show that each $\tilde{\mathcal{B}}_a$ is a two-point LO Feynman graph, i.e. taking $\tilde{\mathcal{B}}_a$ and connecting the two external propagators (i.e. the ones adjacent to v_a and to w_a) yields a LO Feynman graph $\mathcal{B}_a$. Using (4.1) this means that we have to show that $g((\mathcal{B}_a)_{(0kl)}) = 0$ for all pairs of colors k, l. Fix a pair of colors k, l. We know that $\mathcal{B}_{(0kl)}$ is a planar 3-bubble. Hence, as before, we get an embedding defined by the cyclic ordering of the incident edges of each vertex such that no edges overlap. Since v_1 and w_1 are connected by a propagator, this means that they have opposite cyclic ordering of the incident edges. In inset (d) we have chosen one of the two choices for this cyclic ordering, the reasoning for the other choice is analogous. One sees that the opposite cyclic ordering of v_1 and w_1 implies that v_a and w_a also have opposite cyclic ordering. This is illustrated by either of the two possible situations in inset (d). Hence, when connecting the external propagators of $(\tilde{\mathcal{B}}_a)_{(0kl)}$ and deleting the

rest of the graph outside $(\tilde{\mathcal{B}}_a)_{(0kl)}$, we are left with a planar embedding of $(\mathcal{B}_a)_{(0kl)}$ where the faces are the faces of alternating colors. This means that $g((\mathcal{B}_a)_{(0kl)}) = 0$, finishing the proof. □

We are now ready to prove the main result of this chapter, Theorem 4.1.

Proof of Theorem 4.1. We proceed by complete induction on the number of interaction bubbles v in a LO Feynman graph $\mathcal{B}$.

Note that a LO Feynman graph cannot have only one interaction bubble, since then all the propagators connect vertices within the same interaction bubble, which is not allowed by Lemma 4.6. The elementary mirror melon associated with the interaction bubble $\mathcal{K}_n$ is a LO Feynman graph with two interaction bubbles. In fact, this is the only LO Feynman graph with two interaction bubbles, which follows directly from Proposition 4.9: if A, B are the only interaction bubbles, then all $\tilde{\mathcal{B}}_a$ must be equal to the propagator, yielding the elementary mirror melon. We conclude that all LO Feynman graphs with $v = 1, 2$ are melonic.

Assume the theorem is true for all LO Feynman graphs with $v < v_0$ for some fixed $v_0 \geq 3$ and let $\mathcal{B}$ be a LO Feynman graph with v_0 vertices. Proposition 4.9 gives the structure of this graph. Each of the two-point LO Feynman graphs $\tilde{\mathcal{B}}_a$ does not contain A, B, and therefore has at most $v_0 - 2$ interaction bubbles. Hence by the induction hypothesis the LO Feynman graphs $\mathcal{B}_a$ are melonic. Also, there exists at least one $\tilde{\mathcal{B}}_{a_0}$, connected between equivalent vertices v_{a_0} and w_{a_0}, which is a propagator.

We now explain how to obtain $\mathcal{B}$ by repeated insertions of the elementary mirror melon, beginning with the propagator loop. Start with an elementary mirror melon and call one interaction bubble A and the other B, and label the vertices $v_1, \ldots, v_n$ and $w_1, \ldots, w_n$ as in $\mathcal{B}$. Then, cut open the propagator between v_{a_0} and w_{a_0} in the elementary mirror melon and insert into the propagator loop. For each of the remaining propagators between v_a and w_a, $a \neq a_0$, we can perform the same insertions of the elementary mirror melon that are needed to obtain $\tilde{\mathcal{B}}_a$. Ultimately, this process will yield $\mathcal{B}$, hence $\mathcal{B}$ is melonic. □

4.3 MST Colorings and Latin Squares

This section will review what is known about MST colorings and explain the relation to latin squares.

4.3.1 MST Colorings

An MST coloring of a graph is known in the scientific literature as a perfect 1-factorization. We collect some facts from [7], [8] on what is known about perfect 1-factorizations, which is an active area of research. First we define some terminology.

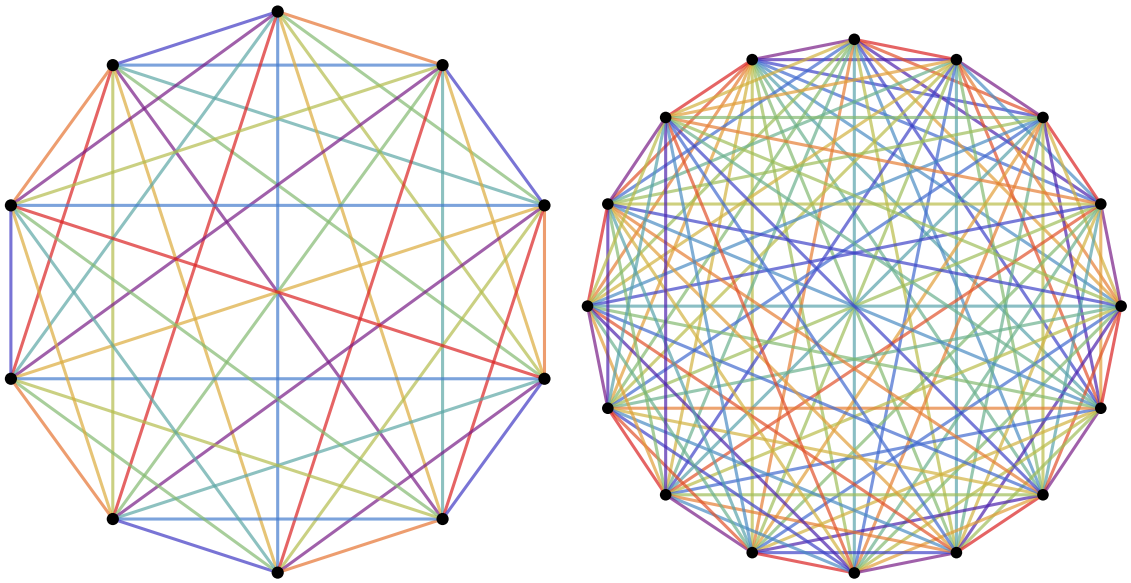

Figure 4.4: The unique (up to isomorphism) MST coloring of the complete graph K_{10} (left) and one of the 3155 (up to isomorphism) MST colorings of K_{16} (right). These are examples of interaction terms for which all LO Feynman graphs are generated by the elementary mirror melon of the interaction.

Definition 4.10. Let G be a graph. A 1-*factor* of G is a subset F of edges of G that are pairwise disjoint (i.e. no two edges in F are incident on the same vertex) such that every vertex in G has an edge in F incident on it. A 1-*factorization* of G is a partition of the edges of G consisting of 1-factors. A 1-factorization is *perfect* if the union of any two 1-factors in the 1-factorization defines a cycle that visits all the vertices in G.

One checks that the notions of MST coloring and perfect 1-factorization coincide: each color corresponds to a 1-factor and the fact that every (ij)-face visits all the vertices corresponds to the fact that the union of every two 1-factors defines a cycle visiting all vertices.

Since we proved that MST colorings of the complete graph yield melonic Feynman graphs, we naturally want to know if such colored graphs exist. And if they exist, how many there are. Perfect 1-factorizations on the complete graph K_n can only exist for even n. Whether or not a perfect 1-factorization of K_n exists for all even n is an open problem, but evidence suggests that this is the case, and their existence was conjectured by Anton Kotzig.

There exist three different constructions of perfect 1-factorizations of K_n for an infinite number of n: two constructions that work for $n-1$ equal to a prime, and one that works for $n = 2p$, with p a prime. For the rest, there exist sporadic examples of perfect 1-factorizations of K_n for n, using different methods. For all even $n \leq 54$ there exists a perfect 1-factorization of K_n, but $n = 56$ is the smallest n for which the existence is still an open question. Note that one of the two constructions for $n-1$ equal to a prime is used in [4] as the interaction term.

It is also interesting to look at the number of non-isomorphic perfect 1-factorizations of K_n that exist for fixed n. For $n = 2, 4, 6, 8, 10, 12, 14, 16$ this is known to be $1, 1, 1, 1, 1, 5, 23, 3155$. See Figure 4.4 for examples of perfect 1-factorizations of K_{10} and K_{16}.

4.3.2 Latin Squares

In the following we will show that a colored complete graph $\mathcal{K}_{n+1}$ for any $n \in \mathbb{N}$ can be represented by an $n \times n$-matrix $\mathcal{L}(\mathcal{K}_{n+1})$, called a latin square. The MST condition on K_{n+1} will be shown to be equivalent to a certain condition on its corresponding latin square. This is based on Theorems 1 and 2 in [9].

Definition 4.11. Let $n \in \mathbb{N}$ and Σ be a set of size n. The elements of Σ are called *symbols*. A *latin square of order* n is an $n \times n$-matrix with entries in Σ such that every symbol appears exactly once in every row and every column.

Let L be a latin square. For any $k \in \Sigma$ the permutation τ_k is defined by $\tau_k(i) = j$ if $L_{i,j} = k$ (i.e. L has entry k in row i and column j). This is indeed a permutation by the properties of a latin square. Next, for any $k, l \in \Sigma$ define the permutation $\sigma_{k,l} := \tau_k \circ \tau_l^{-1}$.

Any permutation can be written as a composition of cycles. We will call $\sigma_{k,l}$ *Hamiltonian* if it consists of just one n-cycle. If $\sigma_{k,l}$ is Hamiltonian for all symbols k, l, then L is called *symbol-Hamiltonian*.

Next, we show how one can associate a latin square to a colored complete graph. For this it is necessary that the colored complete graph is *rooted*, meaning that one vertex is singled out and called the *root*. We also require that there is some ordering on the remaining vertices.

Definition 4.12. Let $\mathcal{K}_{n+1}$ be a coloring of the complete graph K_{n+1}, with v the root, and an ordering on the remaining vertices. Define the latin square $L = \mathcal{L}(\mathcal{K}_{n+1})$ of order n as follows. The symbols Σ are the vertices of $\mathcal{K}_{n+1}$ except v. Label the rows and columns by the symbols in Σ, with the ordering inherited from the ordering of the vertices. For a symbol k, let c be the color of the edge that connects k to v. For all pairs of vertices i, j connected by the color c, set $L_{i,j} = k$. Also set $L_{k,k} = k$.

The following theorem shows that the symbol-Hamiltonian property is the condition on a latin square that is equivalent to the MST condition on a colored complete graph.

Theorem 4.13. *Let $\mathcal{K}_{n+1}$ be a coloring of the complete graph K_{n+1} with root v and an ordering on the remaining vertices. Then $\mathcal{K}_{n+1}$ is MST if and only if $\mathcal{L}(\mathcal{K}_{n+1})$ is symbol-Hamiltonian.*

Proof. "⇒": Let k, l be distinct symbols of $\mathcal{L}(\mathcal{K}_{n+1})$, and let c, d be the colors of the edges connecting v to k, l, respectively. Since $\mathcal{K}_{n+1}$ is MST, there is a single (c, d)-face that passes through all vertices:

$$v \overset{c}{-} (w_1 = k) \overset{d}{-} w_2 \overset{c}{-} w_3 \cdots w_{n-1} \overset{c}{-} (w_n = l) \overset{d}{-} v, \tag{4.16}$$

where $w_1, \ldots, w_n$ are all the vertices besides v. It follows from Def. 4.12 that for $m = 1, \ldots, \frac{n-1}{2}$:

$$\tau_l(w_{2m}) = w_{2m-1}, \quad \tau_k(w_{2m}) = w_{2m+1}, \tag{4.17}$$

hence:

$$\sigma_{k,l}(w_{2m-1}) = (\tau_k \circ \tau_l^{-1})(w_{2m-1}) = w_{2m+1}. \tag{4.18}$$

For $m = 2, \ldots, \frac{n-1}{2}$ we have:

$$\tau_l(w_{2m-1}) = w_{2m}, \quad \tau_k(w_{2m-1}) = w_{2m-2}, \tag{4.19}$$

hence:

$$\sigma_{k,l}(w_{2m}) = (\tau_k \circ \tau_l^{-1})(w_{2m}) = w_{2m-2}. \tag{4.20}$$

Also, $\tau_l(w_n) = w_n$ and $\tau_k(w_n) = w_{n-1}$, hence $\sigma_{k,l}(w_n) = w_{n-1}$.

From the above we see that if we repeatedly apply $\sigma_{k,l}$ starting with w_1, we visit the symbols in the following order:

$$w_1, w_3, w_5, \ldots, w_n, w_{n-1}, w_{n-3}, w_{n-5}, \ldots, w_2, \tag{4.21}$$

hence all symbols are visited. This implies that $\sigma_{k,l}$ consists of a single n-cycle, hence is Hamiltonian. We conclude that $\mathcal{L}(\mathcal{K}_{n+1})$ is symbol-Hamiltonian.

"$\Leftarrow$": Let c, d be two colors of $\mathcal{K}_{n+1}$, and let k, l be the vertices (symbols of $\mathcal{L}(\mathcal{K}_{n+1})$) connected to v by the edges of color c, d, respectively. Since $\sigma_{k,l}$ consists of a single n-cycle, repeated application of $\sigma_{k,l}$ starting with the symbol k will visit every symbol once (hence all vertices of $\mathcal{K}_{n+1}$ except v) in some order:

$$w_0 = k, w_1, w_2, \ldots, w_{n-1}, \tag{4.22}$$

where $\sigma_{k,l}(w_i) = w_{i+1}$ and $w_i \neq k$ for $i \neq 0$. Note that since $\sigma_{k,l} = \tau_k \circ \tau_l^{-1}$, this means that for $w_i \neq l$, the vertex w_i is connected to some vertex u_{i+1} by an edge of color d and u_{i+1} is connected to w_{i+1} by an edge of color c. Hence by repeated application of $\sigma_{k,l}$ starting with k and until we reach l gives the following (c, d)-face in $\mathcal{K}_{n+1}$:

$$v \overset{c}{-} k \overset{d}{-} u_1 \overset{c}{-} w_1 \cdots u_{m-1} \overset{c}{-} w_{m-1} \overset{d}{-} u_m \overset{c}{-} l \overset{d}{-} v. \tag{4.23}$$

Note that $\sigma_{k,l}(l) = \tau_k(l)$, hence $\sigma_{k,l}(l)$ is connected to l by an edge of color c. From the path above we see that we must have $\sigma_{k,l}(l) = u_m$. Similarly we see that we must have $\sigma_{k,l}(u_m) = u_{m-1}$ and repeated application of $\sigma_{k,l}$ will visit $u_{m-2}, \ldots, u_1$. Finally, $\sigma_{k,l}(u_1) = k$, where we started. Since we visit all symbols by repeated application of $\sigma_{k,l}$, we deduce that $k, w_1, \ldots, w_{m-1}, l, u_m, u_{m-1}, \ldots u_1$ are all the vertices of $\mathcal{K}_{n+1}$ except v. Hence the (c, d)-face (4.23) visits all vertices. We conclude that $\mathcal{K}_{n+1}$ is MST. □

5 The Large N, D Limit for Fixed Ratio

In this chapter we introduce a new procedure for taking the large N, D limit. Instead of just taking $N \to \infty$ first and then $D \to \infty$, we keep the ratio of some power of D and N fixed while taking the limits:

$$\frac{D^q}{N} = c, \tag{5.1}$$

where $q, c \in \mathbb{R}$. This will select different Feynman graphs in case $r = 1$, as we will see below.

5.1 Taking the Limit

Recall the expression for the free energy (3.25):

$$F = N^2 D^r \sum_{h,\ell \in \mathbb{N}_0} N^{-h} D^{h - \frac{\ell}{r+1}} F_{h,\ell}. \tag{5.2}$$

Here, $F_{h,\ell}$ contains the contribution of all Feynman graphs with parameters h, ℓ, and is independent of N and D. Also, r is the number of tensor indices. Note that $\ell \geq h$ for any Feynman graph.

Using the fixed ratio (5.1), the free energy becomes:

$$F = N^2 D^r \sum_{h,\ell \in \mathbb{N}_0} c^h D^{h(1-q) - \frac{\ell}{r+1}} F_{h,\ell}. \tag{5.3}$$

In order for the limit $D \to \infty$ to exist there must be an upper bound on the powers of D appearing in the terms above. Taking this limit then amounts to selecting the term(s) with the maximal power of D. Whether the limit exists depends on whether q is greater or less than $\frac{r}{r+1}$:

- **Limit exists for $q \geq \frac{r}{r+1}$.** Using $h \leq \ell$:

$$h(1-q) - \frac{\ell}{r+1} \leq \ell(1 - q - \frac{1}{r+1}) \leq \ell(1 - \frac{r}{r+1} - \frac{1}{r+1}) = 0, \tag{5.4}$$

  hence 0 is the maximal power of D.

- **Limit does not exist for $q < \frac{r}{r+1}$.** If $h = \ell$:

$$h(1-q) - \frac{\ell}{r+1} = \ell \underbrace{\left(1 - q - \frac{1}{r+1}\right)}_{>1-\frac{r}{r+1}-\frac{1}{r+1}=0}, \tag{5.5}$$

  hence the power of D can get arbitrarily large.

Hence we will assume $q \geq \frac{r}{r+1}$ in the following.

Notice that after taking the limit $D \to \infty$ the $h, \ell = 0$ term always contributes to the free energy, irrespective of q. We show that this is in fact the only term that contributes, unless q is precisely equal to $\frac{r}{r+1}$.

- $q > \frac{r}{r+1}$**:** For any h, ℓ not both equal to 0 we have $\ell \neq 0$ (since $h \leq \ell$), and therefore the inequality in (5.4) becomes strict. This means that only the $h, \ell = 0$ term survives:

$$F = N^2 D^r F_{0,0}. \tag{5.6}$$

- $q = \frac{r}{r+1}$**:** In order for the power of D in the free energy to be 0 we must have:

$$0 = h(1-q) - \frac{\ell}{r+1} = \frac{h-\ell}{r+1}, \tag{5.7}$$

  hence all terms with $h = \ell$ will contribute to the free energy after taking the limit:

$$F = N^2 D^r \sum_{h \in \mathbb{N}_0} c^h F_{h,h}. \tag{5.8}$$

5.2 Finding the LO Feynman Graphs for $q = \frac{r}{r+1}$

We see that only for the choice $q = \frac{r}{r+1}$ we get an extra contribution to the free energy, compared to the simple large N, D limit discussed before, which only yields the $h = \ell = 0$ Feynman graphs. In the case of an MST interaction term we have for any Feynman graph $\mathcal{B}$ that $h = 2g$ and $\ell = 2\,\mathrm{ind}_0(\mathcal{B})$. Hence the condition $h = \ell$ is equivalent to $g = \mathrm{ind}_0(\mathcal{B})$. The free energy then potentially contains contributions from all possible genera.

Note that the value $q = \frac{r}{r+1}$ is exactly on boundary of convergence/divergence of the limit $D \to \infty$ of the free energy (5.3). Higher values of q yield only the $h = \ell = 0$ Feynman graphs, while for lower values the free energy diverges.

It is interesting to characterize all Feynman graphs with $h = \ell$. The simplest case would be to consider MST interaction terms such that this condition becomes $g = \mathrm{ind}_0(\mathcal{B})$. Dario Benedetti et al. [1] work out the same limit as we presented here, but only for the case $r = 1$ (one tensor index). Also, they computed which Feynman graphs satisfy $g = \mathrm{ind}_0(\mathcal{B})$ for one specific interaction term: the tetrahedral interaction, which corresponds to the unique MST coloring of K_4. The Feynman

graphs can then all be generated inductively, like melonic graphs, but the process is more complicated: not only elementary mirror melons have to be inserted, but to get graphs with non-zero genus also so-called ladders have to be inserted in a specific way. Note the two different definitions of ℓ in [4] and [1]: calling ℓ in [4] (same conventions as in this thesis) ℓ_F and ℓ in [1] ℓ_B, one checks that $\ell_F = \ell_B + 2g$.

We now show that when using an MST interaction term, the limit with fixed ratio does not yield any new Feynman graphs when $r \geq 2$. Denote by $\mathcal{F}_g$ the Feynman graphs $\mathcal{B}$ satisfying $g = \mathrm{ind}_0(\mathcal{B})$ for some genus g. We already know something about $\mathcal{F}_0$: all the melonic graphs $\mathcal{M}$ (i.e. all the graphs created by melonic insertions of the elementary mirror melon of the interaction term) satisfy $g = \mathrm{ind}_0(\mathcal{B}) = 0$. In the specific case of an MST *complete* graph we showed that these are also *all* the $g = \mathrm{ind}_0\,\mathcal{B} = 0$ graphs: $\mathcal{M} = \mathcal{F}_0$. But for a generic MST interaction there might be other non-melonic $g = \mathrm{ind}_0(\mathcal{B}) = 0$ graphs: $\mathcal{M} \subset \mathcal{F}_0$. In the following we show that when $r \geq 2$ there are no other LO graphs with genus $g > 0$, i.e. $\mathcal{F}_g = \emptyset$ for all $g > 0$ when $r \geq 2$. In contrast, when $r = 1$ and when using the tetrahedral interaction there exist such higher genus graphs, as shown in [1].

Recall that for a Feynman graph $\mathcal{B}$ in a theory with an MST interaction:

$$\mathrm{ind}_0(\mathcal{B}) = \sum_{i<j} g(\mathcal{B}_{(0ij)}), \tag{5.9}$$

where $g(\mathcal{B}_{(0ij)})$ is the genus of the subgraph consisting of only the propagators and edges of color i, j in $\mathcal{B}$. Recall that the genus g referred to before is actually equal to $g(\mathcal{B}_{(012)})$, i.e. the genus of B if we only consider the propagators and the two matrix indices (colors $1, 2$) contractions. Using (5.9), one sees that the condition $g = \mathrm{ind}_0(\mathcal{B})$ is equivalent to:

$$g(\mathcal{B}_{(0ij)}) = 0 \quad \text{for all distinct colors } i, j \text{ such that } i \neq 1, 2 \text{ or } j \neq 1, 2. \tag{5.10}$$

We now show that there are no Feynman graphs with $g > 0$ satisfying (5.10) when $r \geq 2$. Let $\mathcal{B}$ be a Feynman graph with v copies of an MST interaction term, with n the number of vertices in the interaction term. For any two distinct colors a, b the graph $\mathcal{B}_{(0ab)}$ has $E = \frac{3}{2}nv$ edges, $V = nv$ vertices and $F = F_{0a} + F_{0b} + F_{ab}$ faces. Using Euler's Formula $g(\mathcal{B}_{(0ab)}) = \frac{1}{2}(E - V - F) + 1$ and $F_{ab} = v$ (since $\mathcal{B}$ is MST):

$$g(\mathcal{B}_{(0ab)}) = -\frac{1}{2}(F_{0a} + F_{0b}) + \frac{1}{4}(n-2)v + 1. \tag{5.11}$$

Since $r \geq 2$, there exist two distinct colors i, j both unequal to 1 or 2. Using the equation above, one finds:

$$g(\mathcal{B}_{(01i)}) + g(\mathcal{B}_{(02j)}) = g(\mathcal{B}_{(012)}) + g(\mathcal{B}_{(0ij)}). \tag{5.12}$$

The left hand side equals 0, according to (5.10). Hence $g = g(\mathcal{B}_{(012)}) = 0$, which is what we wanted to show.

6 The Two-Point Function

The two-point function is the sum over all two-point Feynman graphs. Recall that a two-point Feynman graph is a Feynman graph with one propagator cut open. If the Feynman graphs are melonic, then we can use combinatorial methods to calculate the two-point function in zero dimensions. We will treat two such methods, one using trees and Cayley's Formula, and another using the Lagrange Inversion Theorem.

We consider a matrix-tensor theory with an MST interaction term on the complete graph with $n \geq 6$ vertices, with coupling constant λ. Recall that such interaction terms yield melonic Feynman graphs. We require $n \geq 6$ because these interaction terms have distinguishable vertices, as explained on page 25. This has consequences for some combinatorial factors we will encounter. The case $n = 4$ (the tetrahedral interaction) can be treated using the same methods, but has slightly different combinatorial factors since its vertices are not distinguishable. We point out that the combinatorial factors encountered in the literature can differ. As also noted in [4], in some papers these factors sometimes seem to be incorrect. However, correcting these factors often amounts to changing the coupling constant λ to $c\lambda$ for some combinatorial factor c, hence does not drastically change the results.

Both methods will lead to the two-point function expressed as a power series in the coupling constant λ:

$$G = \sum_{k=0}^{\infty} \frac{(nk)!(2n)^k}{k!((n-1)k+1)!}\lambda^{2k}. \tag{6.1}$$

This power series is actually the generating function of two-point melonic Feynman graphs with k insertions. It has a radius of convergence λ_0 equal to:

$$\lambda_0 = \sqrt{\frac{1}{2n}\frac{(n-1)^{n-1}}{n^n}}. \tag{6.2}$$

Consequently, the two-point function diverges when the coupling constant exceeds λ_0.

6.1 Method Using Trees and Cayley's Formula

We will show how to assign a certain tree to a two-point Feynman graph and then use Cayley's Formula, which counts trees with labeled vertices, to calculate the two-point function. By definition, a *tree* is a graph such that for every two vertices there is a unique path for which the two points lie at the beginning and end points of the path. First we state and prove Cayley's Formula, making use of so-called Prüfer sequences.

Theorem 6.1 (Cayley's Formula)**.** *The number of trees with $n \geq 2$ labeled vertices $1, \ldots, n$ such that vertex i has degree d_i is:*

$$\frac{(n-2)!}{\prod_{i=1}^{n}(d_i - 1)!}. \tag{6.3}$$

Proof. Let $S \subset \mathbb{N}$ have $n \geq 2$ elements. We first establish a bijection p_S between the set $\mathcal{T}_S$ of labeled trees with n vertices and labels in S, and the set of sequences $(a_1, \ldots, a_{n-2})$ of length $n-2$, where all $a_i \in S$. (Note that since there are n^{n-2} such sequences, this bijection shows that $|\mathcal{T}_S| = n^{n-2}$.)

Let $T \in \mathcal{T}_S$. Define $a_1, \ldots, a_{n-2}$ as follows. Remove the leaf with the lowest label from T and set a_1 equal to the (unique) vertex adjacent to this leaf. Also remove the edge connecting the removed leaf and a_1. Next, from what remains of T, remove the leaf with the lowest label and set a_2 equal to the vertex adjacent to this leaf. Also remove the edge connecting the removed leaf and a_2. Continue this process until only two vertices are left. This defines the *Prüfer sequence* $p_S(T) = (a_1, \ldots, a_{n-2})$. Observe the following fact, which follows from this construction:

Fact ($*$): If a vertex in T has degree d, then its label appears $d-1$ times in the sequence $p_S(T)$.

To prove that p_S is a bijection (i.e. for every sequence $(a_1, \ldots, a_{n-2})$ with elements in S, there exists a unique $T \in \mathcal{T}_S$ such that $p_S(T) = (a_1, \ldots, a_{n-2})$), we use induction on $n = |S|$. For $n = 2$, note that there is only one labeled tree with 2 vertices and one (empty) sequence, hence this case is true.

To prove that p_S is a bijection for $n \geq 3$, assume it is for $n-1$. Let $(a_1, \ldots, a_{n-2})$ be a sequence with elements in S. Since this sequence has length $n-2$, there are at least two integers in S that do not appear in the sequence. Let b be the smallest integer not appearing in the sequence. By the induction hypothesis there exists a unique $T \in \mathcal{T}_{S\setminus\{b\}}$ such that $p_{S\setminus\{b\}}(T) = (a_2, \ldots, a_{n-2})$. Add to T a leaf b and an edge incident on both b and a_1. Let $T' \in \mathcal{T}_S$ be the resulting tree. Note that b is the leaf with the lowest label in T', by our choice of b and Fact $(*)$ (leaves are precisely the labels that do not appear in the Prüfer sequence). Then, after removal of b and the edge connecting it to a_1 from T' we get back T. Thus by following the procedure to obtain the Prüfer sequence, we find that $p_S(T') = (a_1, \ldots, a_{n-2})$.

To see that T' is the unique tree satisfying $p_S(T') = (a_1, \ldots, a_{n-2})$, note the following. Such a tree has b as leaf with lowest label and after its removal one

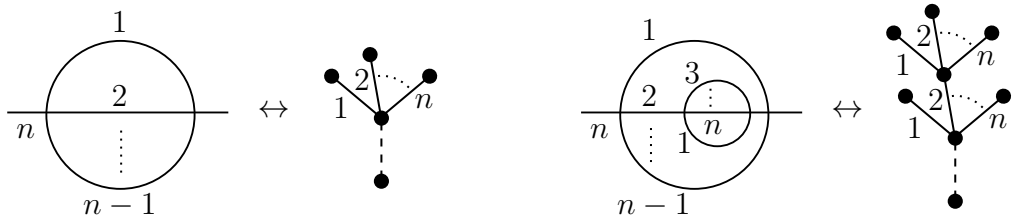

Figure 6.1: Representing melonic Feynman graphs as trees. Every insertion of the elementary mirror melon corresponds to adding n new leaves with labels $1, \ldots, n$, which indicate n possible positions where one can insert another elementary mirror melon. The dashed line indicates the root edge.

obtains a tree in $\mathcal{T}_{S\setminus\{b\}}$ with Prüfer sequence equal to $(a_2, \ldots, a_{n-2})$. This can only be T by our induction hypothesis. We conclude that p_S is bijective.

Fact $(*)$ together with the bijectivity of p_S imply that trees with n labeled vertices with labels in $S = \{1, \ldots, n\}$ and having vertex degrees $d_1, \ldots, d_n$ are in one-to-one correspondence with sequences of length $n-2$ such that label i occurs $d_i - 1$ times, for all $1 \leq i \leq n$. The number of such sequences are:

$$\binom{n-2}{d_1-1}\binom{n-2-(d_1-1)}{d_2-1}\cdots\binom{n-2-(d_1-1)-\ldots-(d_{n-1}-1)}{d_n-1} = \frac{(n-2)!}{\prod_{i=1}^{n}(d_i-1)!}, \tag{6.4}$$

finishing the proof. □

The process of repeatedly inserting an elementary mirror melon to obtain all melonic graphs can be captured by representing melonic Feynman graphs as trees. The propagator (the most simple melonic Feynman graph) is represented by one *root* edge, connecting two vertices. The Feynman graph with one insertion of the elementary mirror melon is represented by the root edge together with n new leaves having labels $1, \ldots, n$. See the left part of Figure 6.1. Here, the labels $1, \ldots, n$ refer to the n different positions on the Feynman graph with one insertion that we can insert a second copy of the elementary mirror melon into. If we insert a copy of the elementary mirror melon into position i, we add n new leaves with labels $1, \ldots, n$ to the leaf labeled i in the tree. For every new copy of the elementary mirror melon we insert, we add n leaves in this way. In the right part of Figure 6.1 we give an example of a Feynman graph with two insertions and its tree. Note that if we want to do a third insertion at position 2 in this graph, then we add n leaves to the leaf 2 that was added during the second insertion.

We have for the two-point function:

$$G = \sum_{k=0}^{\infty} C_k \lambda^{2k}, \tag{6.5}$$

where C_k is the number of melonic two-point Feynman graphs with k insertions of the elementary mirror melon. Consider the structure of the trees representing these

Feynman graphs for some fixed k. One checks that such trees have k vertices with degree $n+1$ (the vertices representing the insertions) and $(n-1)k+2$ vertices with degree 1 (the leaves that are still free for further insertions, and one leaf at the root). According to Cayley's Formula, the number of trees with labeled vertices with these degrees is:

$$\frac{(nk)!}{(n!)^k}. \tag{6.6}$$

However, since we need to count trees with labeled edges and a root vertex and not trees with labeled vertices, we need to compensate with two extra factors. First, since each of the k vertices representing insertions have n labeled edges, we have to multiply with a factor $(n!)^k$. Second, there are $k!$ ways to label the k vertices representing the insertions and $((n-1)k+1)!$ ways to label the $(n-1)k+1$ leaves that are still free for further insertions (note that we fix the one leaf at the root). Hence we have to divide by a factor $k!((n-1)k+1)!$.

Furthermore, note that for every insertion we can choose out of n vertices to cut open in the elementary mirror melon, and can then insert the cut edges in two different ways. Hence we should multiply by a factor $(2n)^k$.

Including these three factors in 6.6, we conclude:

$$C_k = \frac{(nk)!}{(n!)^k}\frac{(n!)^k(2n)^k}{k!((n-1)k+1)!} = \frac{(nk)!(2n)^k}{k!((n-1)k+1)!}. \tag{6.7}$$

6.2 Method Using Lagrange Inversion Theorem

Here we calculate the two-point function by using another method. We will derive the Schwinger-Dyson equation, which is an equation for the two-point function. Then, we will obtain a solution by using the Lagrange Inversion Theorem, which we state here. A proof can be found in e.g. [10].

Theorem 6.2 (Lagrange Inversion Theorem)**.** *Let $\phi(u)$ be a formal power series in u such that $\phi(0) = 1$. Then there exists a unique formal power series $u(t)$ such that:*

$$u(t) = t\phi(u(t)). \tag{6.8}$$

Furthermore, for this solution the coefficients c_k of $f(u(t)) = \sum_{k=0}^{\infty} c_k t^k$, where $f(u)$ is any formal power series in u, are given by:

$$c_k = \frac{1}{k!}\frac{d}{du^{k-1}}\left(f'(u)(\phi(u))^k\right)\Big|_{u=0}. \tag{6.9}$$

First, we derive the Schwinger-Dyson equation. Below, we represent the two-point function G by a gray circle with two outgoing propagators. The most simple two-point Feynman graph is the propagator itself. All other Feynman graphs contain at least one insertion of the elementary mirror melon. We can obtain all graphs

having at least two insertions by starting with the graph with one insertion and then doing insertions on n different positions. This leads to the following equation:

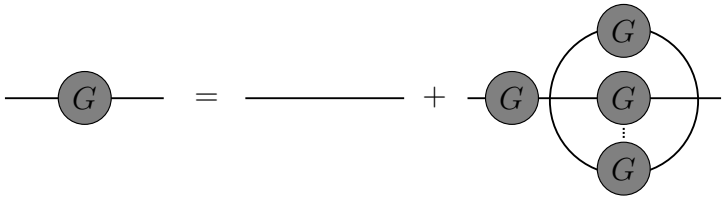

(6.10)

Note that we have drawn only four copies of G on the right hand side, but it is left implicit (by the dots) that there should be n copies. In symbols, this equation is:

$$G = 1 + n\lambda^2 G^n. \tag{6.11}$$

Here, the factor $2n$ takes into account that for every insertion there are n propagators in the elementary mirror melon that we can cut and then two ways to attach the cut edges.

The Schwinger-Dyson equation in this form is different from the equation solved by the Lagrange Inversion Theorem. Therefore, we derive an equivalent equation in a form such that we can apply this theorem, using the self-energy Σ defined as:

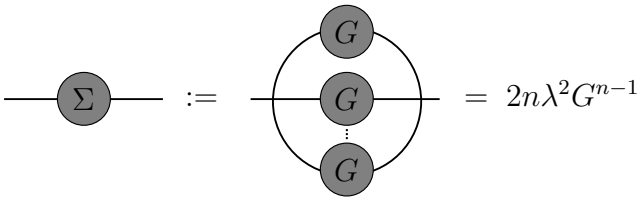

(6.12)

Then:

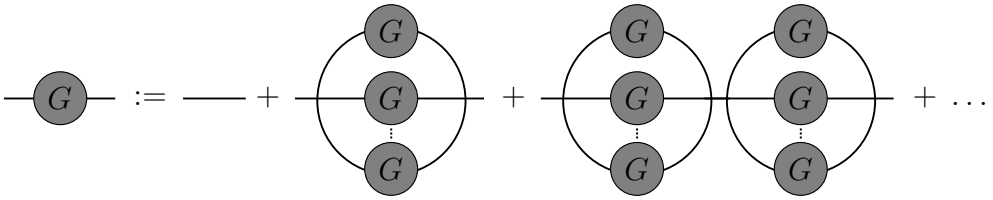

(6.13)

Or in symbols:

$$G = 1 + \Sigma + \Sigma^2 + \ldots = (1 - \Sigma)^{-1}. \tag{6.14}$$

Combining this with (6.12), we find:

$$\Sigma = \frac{2n\lambda^2}{(1-\Sigma)^{n-1}}. \tag{6.15}$$

This equation is of the form needed to use the Lagrange Inversion Formula: using $\phi(u) = (1-u)^{-n+1}$, $f(u) = (1-u)^{-1}$, $u = \Sigma$, $t = 2n\lambda^2$ we can compute the

coefficients in the power series expansion $f(u(t)) = \sum_{k=0}^{\infty} c_k t^k$:

$$\begin{aligned} c_k &= \frac{1}{k!} \frac{d}{du^{k-1}} \left((1-u)^{-2-nk+k} \right) \Big|_{u=0} \\ &= \frac{1}{k!}(nk-k+2)(nk-k+3)\cdots(nk) \\ &= \frac{(nk)!}{k!((n-1)k+1)!}. \end{aligned} \tag{6.16}$$

Since $G = f(u(t)) = \sum_{k=0}^{\infty} C_k \lambda^{2k}$, we have:

$$C_k = (2n)^k c_k = \frac{(nk)!(2n)^k}{k!((n-1)k+1)!}, \tag{6.17}$$

which is the same as obtained by the method using Cayley's Formula.

6.3 Attempting to Solve for Non-Zero Dimension

We make two attempts at computing the two-point function in the case of non-zero dimension. In the first method, we introduce an operator that encodes the integrations over spacetime involved for non-zero dimension, and rewrite the Schwinger-Dyson equation. A second method involves discretizing spacetime in one dimension and writing down the equations from the first method in this setting.

6.3.1 Using an Operator on Functions

Unlike the Schwinger-Dyson equation in zero dimensions (6.11) or (6.15), this equation in higher dimensions involves integrals over spacetime. Also, the two-point function $G(x_1, x_2)$ and the quantity $\Sigma(x_1, x_2)$ now depend on two spacetime points x_1, x_2 (but note that by translational symmetry they actually only depend on the difference $x_2 - x_1$). We will write the Schwinger-Dyson equation in a form involving some kind of operator, but it's not clear how to solve the equation.

Define the following function in two spacetime points:

$$\Sigma(x_1, x_2) = 2n\lambda^2 (G(x_1, x_2))^{n-1}. \tag{6.18}$$

Let $G_0(x_1, x_2)$ be the propagator. Define the linear operator $\mathcal{O}$ on the space of functions in two spacetime points by:

$$(\mathcal{O}f)(x_1, x_2) = \iint dydz G_0(x_1, y)\Sigma(y, z) f(z, x_2), \tag{6.19}$$

where f is any function in two spacetime points and both integrals are over spacetime. Intuitively, this means that we "glue" a propagator and Σ to one side of f

and integrate the two new vertices inside Σ over spacetime. Pictorially:

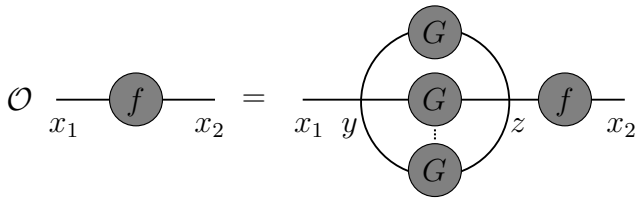

(6.20)

Using the fact that melonic insertions generate all the LO Feynman graphs, one finds:

$$G(x_1, x_2) = G_0(x_1, x_2) + (\mathcal{O}G_0)(x_1, x_2) + (\mathcal{O}^2 G_0)(x_1, x_2) + \dots. \tag{6.21}$$

Recognizing this as the geometric series, we find:

$$G = (\mathcal{I} + \mathcal{O} + \mathcal{O}^2 + \dots)G_0 = (\mathcal{I} - \mathcal{O})^{-1} G_0, \tag{6.22}$$

where $\mathcal{I}$ is the identity operator. Here we assume that it is possible to use the formula for the geometric series for $\mathcal{O}$. Another way to arrive at this equation is to observe the following, where we use that applying $\mathcal{O}$ to G yields all Feynman graphs with at least one insertion (hence all graphs except the propagator):

$$(\mathcal{O}G)(x_1, x_2) = G(x_1, x_2) - G_0(x_1, x_2), \tag{6.23}$$

from which (6.22) follows. Inserting (6.22) into (6.18):

$$\Sigma = 2n\lambda^2((\mathcal{I} - \mathcal{O})^{-1} G_0)^{n-1}. \tag{6.24}$$

Inserting this into (6.19):

$$(\mathcal{O}f)(x_1, x_2) = 2n\lambda^2 \iint dydz G_0(x_1, y)(((\mathcal{I} - \mathcal{O})^{-1} G_0)(y, z))^{n-1} f(z, x_2). \tag{6.25}$$

6.3.2 Discretizing Spacetime, Case of One Dimension

We now consider the case of one dimension and discretize spacetime into N spacetime points $x_1, x_2, \dots, x_N$, where $x_{i+1} - x_i = \Delta$. We will rewrite the formulas of the previous section in a discretized form. Σ is now an $N \times N$-matrix defined in analogy with (6.18):

$$(\Sigma)_{x_i, x_j} = 2n\lambda^2 (G_{x_i, x_j})^{n-1}. \tag{6.26}$$

$\mathcal{O}$ is now a linear operator on the space of $N \times N$-matrices, and integration becomes summation. In analogy with (6.19), $\mathcal{O}$ is defined by:

$$(\mathcal{O}f)_{x_i, x_j} = \sum_k \sum_l (G_0)_{x_i, x_k} (\Sigma)_{x_k, x_l} (f)_{x_l, x_j} = (G_0 \Sigma f)_{x_i, x_j}, \tag{6.27}$$

where f is any $N \times N$-matrix. Hence, $\mathcal{O}$ is just left multiplication by $G_0\Sigma$. Then, the analogue of (6.21) and (6.22) is:

$$G = G_0 + \mathcal{O}G_0 + \mathcal{O}^2 G_0 + \dots = (I - G_0\Sigma)^{-1} G_0. \tag{6.28}$$

Inserting this into (6.26):

$$\Sigma = 2n\lambda^2((I - G_0\Sigma)^{-1}G_0)^{(n-1)}. \tag{6.29}$$

Here, the $(n-1)$ in the superscript of the matrix means that we take every entry in the matrix to the power $n-1$ (and not the power $n-1$ of the matrix by matrix multiplication).

7 Conclusions and Outlook

In this thesis we were able to show that a certain general set of interaction terms leads to melonic Feynman graphs in the matrix-tensor model proposed by Ferrari et al. These melonic graphs appear in both tensor models and the SYK model, and are believed to be able to capture the physical description of quantum black holes.

Besides the new set of interaction terms, we also touched upon two other topics: a different large N, D limit and combinatorial methods to compute the two-point function in zero dimensions.

We saw that for the case of MST interactions, the different large N, D limit does not yield anything new as compared to the standard limit when the number of tensor indices is at least two. However, when the number of tensor indices is one, this limit does potentially yield interesting new Feynman graphs, besides the melonic graphs. This was explored only for the case of the tetrahedral interaction in [1]. A potential direction for future research would be to consider other MST interaction terms using one tensor index. These types of terms might yield non-melonic Feynman graphs similar to those in [1], containing ladders or a generalization thereof.

The generating function associated with two-point melonic Feynman graphs (6.1) has a finite radius of convergence (6.2), implying that the two-point function diverges for a sufficiently large coupling constant. As seen in [1], generating functions associated with more complex Feynman graphs (e.g. involving ladders) can also show this kind of behavior. It would be interesting to explore similar behavior if we are able to compute the Feynman graphs in a theory with one tensor index and an MST interaction term different from the tetrahedral term.

The two-point function in zero dimensions is particularly easy to solve using combinatorial methods (Cayley's Formula for trees and the Lagrange Inversion Theorem). We made an effort to rewrite the Schwinger-Dyson equation for the case of non-zero dimension in two different ways: by introducing an operator that encodes the integration over spacetime that has to be performed for higher dimensions, and by discretizing spacetime in one dimension. One could try to solve these equations by (the higher dimensional version of) the Lagrange Inversion Theorem. Progress in this direction would give another way to compute the two-point function, besides the numerical Fourier transform method that is often used.

Acknowledgments

First and foremost, I'd like to thank my supervisors Umut Gürsoy and Ivan Kryven for their guidance in this project. Also, I want to thank them for their support in helping me get a PhD position.

Thanks also to Natale Zinnato, Eric Marcus and Ronnie Rodgers for their input during all our meetings.

Finally, many thanks to my parents for supporting me during my work on this thesis, especially towards the end.

Bibliography

[1] Dario Benedetti, Sylvain Carrozza, Reiko Toriumi, and Guillaume Valette. Multiple Scaling Limits of $\mathrm{U}(N)^2 \times \mathrm{O}(D)$ Multi-Matrix Models. 2020.

[2] Sylvain Carrozza and Adrian Tanasa. $\mathrm{O}(N)$ Random Tensor Models. *Lett. Math. Phys.*, 106(11):1531–1559, 2016.

[3] Frank Ferrari. The Large D Limit of Planar Diagrams. *Annales de l'Institut Henri Poincaré D*, 6(3):427–448, 2019.

[4] Frank Ferrari, Vincent Rivasseau, and Guillaume Valette. A New Large N Expansion for General Matrix–Tensor Models. *Commun. Math. Phys.*, 370(2):403–448, 2019.

[5] Alexei Kitaev. *A Simple Model of Quantum Holography*, 2015. `https://online.kitp.ucsb.edu/online/entangled15/`.

[6] Bojan Mohar and Carsten Thomassen. *Graphs on Surfaces*. John Hopkins University Press, 2001.

[7] Alexander Rosa. Perfect 1-factorizations. *Mathematica Slovaca*, 69(3):479 – 496, 2019.

[8] Ian M. Wanless. *Perfect* 1*-factorisations*, Accessed 15-11-2020. `http://users.monash.edu.au/~iwanless/data/P1F/newP1F.html`.

[9] Ian M. Wanless and Edwin C. Ihrig. Symmetries That Latin Squares Inherit from 1-Factorizations. *Journal of Combinatorial Designs*, 13(3):157–172, 2005.

[10] Herbert S. Wilf. *generatingfunctionology*. 1994. `www.math.upenn.edu/~wilf/gfologyLinked2.pdf`.

[11] Edward Witten. An SYK-Like Model Without Disorder. *Journal of Physics A: Mathematical and Theoretical*, 52(47):474002, 2019.